Financial Networks and Interconnectedness in an Advanced Emerging Market Economy

Ariel J. Sun and Jorge A. Chan-Lau *

November 2016

Abstract

Financial networks could become fragile during periods of economic and financial distress, since interconnectedness among participating firms could transmit and amplify adverse shocks. Relying on balance sheet data, complemented with information on interbank exposures, this paper analyzes interconnectedness in an advanced emerging market economy, using two complementary approaches. The first approach focuses on the financial network topology, and finds that the financial system resembles a highly clustered *small world* network, with in and out-degree, connectivity, and exposures exhibiting a (double) heavy tail behavior, which favors the formation of strong community structure and *preferential attachment* in the network. The second approach focuses on how the network topology contributes to the transmission of shocks modeling default contagion, using balance-sheet network analysis. It finds that direct counterparty credit exposure poses less risk to the banking system than fire-sale losses triggered by liquidity shocks. Both approaches, either using a topological or induced system losses perspective, identify systemically important financial institutions (SIFIs) consistently by accounting for both macro and microprudential risk dimensions.

Keywords: banking system, emerging market, contagion, systemic risk, interconnectedness, interbank network, centrality, macroprudential, microprudential

Authors' emails: js308@imperial.ac.uk (corresponding author); jchanlau@imf.org

*Ariel J. Sun is a PhD Candidate in Finance at Imperial College Business School, Imperial College London; Jorge A.Chan-Lau is a senior economist at the International Monetary Fund (IMF). This paper, partially written while Sun was an intern at the IMF, won the Best Paper Award (Best Applied Paper) at the 4th European Conference on Banking and the Economy (ECOBATE 2016), Winchester, UK. The authors would like to thank seminar participants there, as well as those at the IMF, the 2nd Young Finance Scholars' Conference (Quantitative Finance Workshop) at University of Sussex, UK, May 2014; 2nd RiskLab/BoF/ECB/ESCB Conference on Systemic Risk Analysis in Helsinki, Finland, Oct 2016 for their valuable comments and feedback. We benefitted greatly from the invaluable advice offered by Rustam Ibragimov, Professor of Finance and Econometrics, Imperial College Business School, Imperial College London. The authors bear all responsibility for remaining errors. The views expressed here are those of the authors and do not represent those of the IMF nor IMF policy.

Contents

1 Financial Crisis and Interconnectedness Risk

Financial crises, unfortunately, tend to occur more frequently than expected and seemingly without prior warning. During the post-second world war period, the global economy has been shaken by several financial

crises, including but not limited to the debt crisis in Latin America in the 1980s, the breakdown of the European Monetary System and the collapse of the Scandinavian banking system in the early 1990s, the Asian crisis in 1997, followed by the Russian debt default in 1998. The later contributed to the demise of Long Term Capital Management (LTCM), a relative value hedge fund, prompting its bailout by its major private sector counter-parties. The bailout, organized by the Federal Reserve Bank of New York, aimed at assuaging concerns about the negative spillovers from a disorderly unwinding of LTCM's highly levered positions and its contagion on related counter-parties, through losses arising from direct exposures, and also on unrelated counter-parties, from the downward pressure on funding liquidity affecting the market value of securities holdings and the ability to roll over short-term funding (Brunermeier and Pedersen, 2009 [14]).

The demise of LTCM was a prelude to the global financial crisis in 2007-8, which highlighted dramatically the dangers of interconnectedness risk poses to the financial system. The origins of the crisis could be traced back to a surge of defaults in the subprime mortgage market in the United States, following a decline in house prices in major urban areas. Given the relatively small size of the market, the policy making community believed that problems were likely to be contained in the area, as Chairman Bernanke suggested in his testimony to the U.S. Congress in 2007. With the benefit of hindsight, this sanguine assessment ignored several factors, all of them linked to interconnectedness in the financial system, that amplify the initial shocks and led to a major crisis which ultimately engulfed all major financial institutions. These factors include:.

1. Increased cross-border linkages, which facilitated major international shock spillovers. Haldane (2009) [33], documents a fourteen-fold increase in cross-border stocks of external assets and liabilities in eighteen advanced economies, measured relative to GDP, from 1985 to 2005.

2. Heavy reliance on complex financial instrument, which contributed to higher leverage in the financial system and the amplification of default losses. In the run-up to the global recession, the prevailing low rate environment encouraged market participants to boost the profitability of their investment strategies through the use of collateralized lending including repurchase agreement (REPO) and reverse REPO operations, collateralized debt obligations (CDO), mortgage-backed securities (MBS), and asset-backed securities (ABS). This trend, in turn, led to heightened complexity in financial markets, making it more difficult for regulators to assess the extent of exposures and embedded leverage both at the system or macro-level, and at the firm or micro-level.

3. Heightened homogeneity, driven by the adoption of similar investment strategies as market participants searched for yield and further encouraged by regulatory requirements inducing similar risk management practices across institutions. In the face of an adverse shock, homogeneous firms react similarly. The ensuing herd behavior could lead to a disorderly unwinding of exposures, and the fire-sale of assets would amplify the initial shock, therefore affect market and funding liquidity adversely.

4. Inadequate understanding of the interaction between credit risk, market risk and funding risk, which prevented market participants and authorities from assessing adequately default contagion and its impact on liquidity and funding conditions. The situation was aggravated by the complexity of the instruments being used, and no prior similar historical experience.

The linkage between financial crises and interconnectedness risk motivates this paper, which analyzes it in the context of an advanced emerging market economy. We approach the analysis from two different

perspectives. The first perspective emphasizes the topological properties of the financial network in the economy; the second perspective uses a simulation approach to analyze default contagion based on balance-sheet network analysis.. Before delving into the analysis it is necessary to frame interconnectedness risk and its measurement within the broader concept of systemic risk, which we do in the next section.

1.1 Systemic Risk and Interconnectedness

The concept of systemic risk is largely associated with the fallout of financial crises, with the latter closely associated with banking panics and the resulting drying up of liquidity in the banking system, and its ultimate impact on real economic activity (Friedman and Schwartz, 1963 [29]). Gorton (2010) [31] offered a more recent iteration, accounting for the interaction between the banking system and the shadow banking system. Along this line of reasoning, Franklin and Mishkin (1995) [23] defined a financial crisis as "(an event that) involves sharp declines in asset prices, failures of large financial and non-financial firms, deflation or disinflation, disruptions in foreign exchange markets." This idea feeds naturally in the definition of systemic risk, advanced in Mishkin (1994) [40]) and Bank of International Settlements (BIS, 1994 [9]), as the risk of potential disruptions to the funding channel and/or to the payment system in the event of a financial crisis triggered by the default or failure of a market participant to honor its obligations. This definition highlights interconnectedness as a source of systemic risk. Along this perspective, the U.S. Commodity Futures Trading Commission defines systemic risk as "the risk that a default by one market participant will have repercussions on other participants due to the interlocking nature of financial markets. Similarly, Kaufman (1995) [36] defined systemic risk as the "chain reaction of falling interconnected dominoes." Finally, the U.S. Federal Reserve relates systemic risk to the disruption of payments system: "... an institution participating on a private large-dollar payments network were unable or unwilling to settle its net debt position ... Serious repercussions could, ... spread to other participants ... , to other depository institutions not participating in the network, and (Board of Governors of the Federal Reserve System (2001) [11]).

But more generally, at least among macroeconomists, disruptions to payment systems or to the financial system may not represent systemic risk, as long as the real economy continues functioning normally. Short-lived stock market crashes such as the one experienced in the United States in October 1987 (Black Monday), or the trillion dollar Flash Crash in May 2010, attributed to high frequency trading (Kirilenko et al, 2014 [37]), did not constitute systemic risk events. Accounting for the impact on the real sector, the Group of Ten (2001) [32] defines systemic risk as "... the event will trigger a loss of economic value ... have significant adverse effects on the real economy." The European Central Bank (ECB), likewise, defines systemic risk as a financial instability risk that is "so widespread that it impairs the functioning of a financial system to the point where economic growth and welfare suffer materially (ECB, 2010 [22]). Billio et al. (2010) [8] define systemic events as "any set of circumstances that threatens the stability of or public confidence in the financial system" while the G-20 defines systemic risk as "disruptions to financial services... could affect the real economy." We conclude this discussion by noting that under a systemic risk perspective, financial regulation and supervision needs to adopt a macro-prudential approach aimed at reducing risks to the financial system as a whole, instead of the traditional micro-prudential approach aimed at mitigating the risks of individual institutions on a stand-alone basis (see Brunnermeier et al, 2009a).

Once we settle on a definition of systemic risk, the next challenge is to measure it. Bisias et al. (2012)[10]

documented more than 30 different ways to measure systemic risk. They can be roughly classified into two categories depending on the nature of the shocks and/or factors affecting the financial system:

1. Type I systemic risk measures assume that financial instability arises endogenously, and can be captured ex-ante by analyzing the interaction and feedback between economic and financial factors. In principle, these measures could help finding early warning signals based on the identification of behavioral patterns in the financial system, including price and trading volume dynamics, that characterizes the build-up of systemic risk.

2. Type II systemic risk measures assume that the failure of single firm or a group of firms generates financial instability though knock-off effects on other firms, due to direct and indirect exposures. Since defaults are typically considered unpredictable events, the measurement of systemic risk in this category relies on what-if scenario analysis attempting to capture the impact of the default of a firm on others.

Within the Type II measures, there are two categories that are of interest from a regulatory standpoint. The first one is the category of Too-Big-to-Fail (TBTF) measures, which evaluate a firm's size relative to the domestic and/or global financial market where it operates, focusing on its market share and substitutability, i.e. whether other firms could provide similar services at a similar price if the firm were to cease operations. TBTF measures assume implicitly that the failure of a dominant firm could pose a substantial threat to the financial system and the markets where the firm operates, given its linkages to other firms, both financial and non-financial, and the importance of the services it provides, (Laconte, 2015 [38], BCBS, 2013 [7]).

The second category comprises Too-Interconnected-to-Fail (TICTF) measures which attempt to capture the likelihood of the failure of a single firm and its effect on the financial sector and the real economy. Focus on these type of measures seems justified, as concerns about interconnectedness risk have shaped the response of government officials in recent crisis episodes, as it was the case of the bailout of the insurance firm American International Group, Inc (AIG) in the aftermath of the bankruptcy of Lehman Brothers in September 2008.

The remainder of the paper, which focuses on TICTF measures, is organized as follows. Section 2 frames the paper's contribution in the extant literature. Section 2.3 presents the key findings. Detailed analysis on network properties can be found in section 3, and default mechanism can be found in section 4. Section 5 concludes. The Appendix (Sec 7) provides additional information.

2 Interconnectedness Risks

2.1 Microprudential and Macroprudential Approaches

To better understand systemic risk, it is appropriate to analyze it from both the micro and macroprudential perspectives. At the microprudential level, the systemic importance of an individual firm in the financial network depends on the size of its balance sheet and its capital reserves relative to the firm's overall exposure to other firms (or interbank exposure if we restrict the analysis to the banking system). At the macroprudential level, which emphasizes the stability of the system as a whole, the topological properties of the network, or interconnectedness among the firms, determine how likely domino effects are, and if triggered, what the

potential damages to the system are. For simplicity, the defaults that trigger the domino effects are assumed as exogenous events in this paper.

When studying the banking network, we used a microprudential *model-free* analysis that assessed how the attributes of individual firms, such as capital buffers and the size of firms, influenced network properties such as the distribution of connectivity measures. The *model-free* approach does not require specifying an explicit default mechanism nor a contagion chain, which makes it particularly useful when detailed balance sheet data and interbank exposure data are unavailable and a specific default contagion mechanism is either unobservable or difficult to discern.

We complemented the microprudential analysis with a macroprudential *model-based* analysis that captured the domino effect or contagion chain triggered by the default of a firm. The default mechanism, based on the observed behavior of financial firms in past crisis events, incorporated various factors contributing to a cascade of failures following an initial default, such as direct counterparty credit exposures, market shocks and liquidity shortages. Hence, the approach captured the macroprudential dimension associated with interconnectedness.

2.2 Related Literature

Several strands of the academic literature and current policy debates influence our study. The *model-free* approach builds on the early work on modern network theory of Newman (2003) [43], which set the foundations for the analysis of the topological properties of financial networks. Together with Boss et al. (2004) [12] and Cont et al (2012) [20], this paper is among the few that analyze the empirical structure of a financial system using real-world, highly disaggregated data on the banking sector of an advanced (emerging) market economy. Having access to disaggregated and complete exposures helps the paper stand out from earlier work using aggregate exposure data. By necessity, the latter relied on maximum entropy methods to infer unobserved bilateral interbank exposures from aggregate counterparty exposures (Sheldon and Maurer, 1998 [47]; Upper and Worms, 2004 [49]; Wells, 2004 [52]; Elsinger et al., 2006a,b [25, 26]; Degryse and Nguyen, 2007 [21]). But as pointed out by Cont et al (2012), maximum entropy methods typically assume exposures are shared equally among all counterparts, which is at odds with data on reported interbank exposures. As a result, maximum entropy-based studies could underestimate the likelihood and severity of contagion and domino effects in financial networks.

Following the earlier network literature, the *model-based* approach builds on a numerical simulation framework, first developed by Eisenberg and Noe (2001) [24], who assumed a fictitious default mechanism to model domino effects; and Furfine (2003) [30], who assumed a more natural sequential default mechanism, i.e. firms default one by one if the losses incurred exhaust their safety buffers. In Eisenberg and Noe (2001) [24], following an initial default, the existence of a unique equilibrium requires all surviving firms to liquidate their cross holdings to determine their equilibrium values, assuming all liabilities receive equal priority. Cont et al. (2012) [20] argue that such equilibrium is unrealistic. Rather, it may be more appropriate to assume that when firms facing a liquidity shortage unwind their portfolios, the recovery rate could be as low as zero in the short-run. This assumption seems consistent with the protracted and lengthy bankruptcy procedures observed in practice, which forces creditors looking forward to cut their exposures rapidly to accept low recovery rates. The sequential default algorithm of Furfine (2003) [30] bypasses Eisenberg and Noe's

equilibrium conditions, modeling instead the potential cascade of failures that a single default could trigger. Furfine applied his algorithm to analyze the U.S. federal funds market. Since this market only comprises around one-seventh of the U.S. wholesale interbank market, the results might have underestimated systemic risk in the U.S. financial system (Upper and Worm, 2004 [49], Armantier and Copeland, 2012 [4]).

Our analysis goes some steps beyond the earlier literature discussed above. As in previous studies, it captures the systemic risk associated with credit risk driven contagion, or *primary effects*. Following a round of initial defaults, or *fundamental default,* the transmission of the initial shock relies only on the credit losses resulting from the failure of debtor banks to honor their obligations. The initial round of credit losses could cause additional banks to fail, triggering subsequent defaults. But our analysis also looks at the *secondary effects* associated with the funding risk and liquidity shortages that occurred when creditor banks demand immediate repayment from failed or stressed debtor banks. The later set of banks, facing higher funding costs, may be forced to sell their assets at fire sale values, which in turn would reduce the fair asset and equity value of banks holding similar assets, creating an adverse positive feedback effect or liquidity spiral (Brunnermeier and Pedersen, 2009b [13]). We capture both *primary* and *secondary effects*, the latter linking funding costs and fire-sale losses to the solvency of individual firms, using an extension of the balance sheet network models of Jo (2012)[35] which in turn builds on the earlier work of Chan-Lau (2010)[15].

Finally, while this study benefits from data availability on interbank exposures, we would like to discuss briefly alternative approaches based on market price data that could make up for the lack of exposure data. For instance, Acharya et al. (2010) [1] and Zhou et al. (2009) [54]construct systemic risk measures based on high frequency historical market data on credit default swap spreads and/or equity return volatility. Chan-Lau et al (2016) [16] identify systemically important banks using partial correlation networks, where the links between firms correspond to the partial correlation of projected probabilities of default. These projections use information from market prices and balance sheet and income statements. One assumption underlying these measures is that markets are sufficiently efficient, ensuring that market prices capture well information on the risk profile of the firms analyzed, including their potential interaction during periods of distress.

2.3 Some Selected Results

While results will be discussed in detail later, this section offers a glimpse of the main results. In this advanced emerging market economy, the network comprised twenty five banks, and any two banks were pairwise connected if there were counterparty exposures between them. These exposures could be related to any of twenty seven different asset classes (see Table 2), differentiated by type of contract, currency of denomination, and maturity. In the analysis, we used counterparty exposure data as of end-September 2010.

From the microprudential perspectives, we have examined several properties of this interbank network:

1. Network topology reveals a semi-complete network exhibiting a high degree of clustering. While the number of potential edges or links in the network, determined by the existence of counterparty exposures, could be as high as three hundred, the number of existent edges was roughly half at about one hundred fifty, with one disconnected node. Completeness, or full interconnectedness, can be a double-edged sword: Allen and Gale (2000) [2] argue that completeness makes the financial network

more resilient by creating multi-dimensional connections among firms, and hence more credit channels; at the same time, this property creates additional transmission channels for shocks during adverse market condition, with one firm's default affecting several firms at the same time.

2. Compared to other financial networks, banks in this economy tend to cluster closely together, exhibiting the *small world* property. The global clustering coefficient of this network, which measures the number of groups of three banks connected to each other, is around$\sim$0.53, well above what has been found for Austria ($\sim$0.12) (Boss et al, 2004 [12]). Boss et al. (2004) [12] also points out that the Austrian network is a *small-world* network, with *three degrees of separation*, meaning the path lengths among the nodes are smaller than three. Originally described by Watts and Strogatz (1998) [51], a *small-world* network can be created by randomly rewiring several links among the nodes of a regular ring lattice graph; these links become the short-cuts among the originally distant nodes, which creates a short average path length of the network. Compared to the Austrian interbank network, another emerging market economy, Brazil, described in Cont et al. (2012) [20], presents decaying local clustering coefficient, across nodes with increasing degrees of connection. Cont et al (2012) [20] argue that, a small diameter (path length) is not sufficient to characterize the *small-world* property. Indeed, the Brazilian financial network does not enjoy the *small world* property since the distribution of the local clustering coefficients across all nodes is not bounded away from zero. In comparison, our network can be characerized as a *samll world* netowrk: it has asignificantly higher local clustering coefficient (see Table 5), only slightly larger path length than that of its random graph counterpart, and *two degrees of separation*, meaning every bank in this network connects to its neighbour through one other bank at most.

3. The financial network exhibits (double) heavy-tailedness: The interbank network can be naturally separated into a core, comprising a reduced number of institutions, and a periphery, comprising the rest, which suggests a multi-money centre structure (Allen and Gale, 2000[2]). This is a natural outcome for a network that exhibits a two-sided heavy-tailed distribution, where the degree measures the number of connections a bank has. The left tail comprises banks with a small number of connections and distant from the core, and mainly groups foreign bank branches. The right tail comprises banks with a large number of connections, and mainly comprises domestic banks. Within the banking system, the right tail banks are the most important (systemic) ones from an economic viewpoint. Two-sided heavy tail distributions also support the existence of a *preferential attachment* effect in the network, or in other words, highly connected notes tend to get more connected as the network expands (Barabasi and Albert, 1997[6]). Our network connectivity and exposure distributions are similar to those of Austrian network (Boss et al. (2004) [12]), which also have double heavy-tailedness. In comparison, Brazilian interbank network connectivity and exposure distributions seem to have significant right tail only (Cont et al., 2012) [20]. In comparison, German interbank network connectivity and exposure distributions, do not exhibit significant heavy-tailedness (Roukny et al., 2014 [46]).

4. Capital ratio: Using capital ratio requirement proposed by Basel III, all banks in this network seem to have adequate buffer. However, when applying relative exposure measures described in Cont et al. (2012) [20], we identify several institutes at the borderline of capital adequacy. Centrality measures also capture the SIFIs in the network in the debt and credit dimensions; in other words, the important debtors and creditors in the banking system.

The microprudential analysis identifies a set of core banks systemically more important than other banks based on their counterparty exposures. The macroprudential analysis then allows us to evaluate whether the failure of a systemic bank could impair the banking system. The sequential default analysis, based on numerical simulations, suggest that despite the core-periphery structure and the incompleteness of the network, bank defaults are likely to remain isolated events and would not trigger a cascade of failures, due to credit risk alone. This result follows from the structure of the banking system, where banks counterparty exposures are small relative to the assets in their balance sheet, and their capital buffers. Credit losses, or *primary effects*, do not seem to be the main source of losses to banks, but rather the losses associated with the *secondary effects*, or fire sale of assets when firms face liquidity shortages. This finding appears consistent with empirical evidence, albeit yet scant, that fire sale of assets tend to drive losses during crises (Mitchell and Pulvino, 2010 [41]; Merrill et al, 2013 [28]), and supports the lender of last resort role played by the central bank. In comparison, it worths mentioning that Upper and Worm (2004) [49] estimate the bilateral exposure in the German banking system, using balance sheet information, and measure the credit risk due to bilateral counterparty exposure. Their results show given the safety net of institutional guarantees for saving banks and cooperative banks, which reduces contagion risks significantly, one single bank default can cause as much as 15% assets destroyed in the entire banking system.

3 Banking Network Topology

3.1 Data

The dataset used in the analysis comprises 25 financial institutions, including 12 domestic banks (DBs) and 13 foreign bank branches (FBs) operating in the domestic market. Among the domestic banks we included global banks since the nature of their operations resemble those of domestic banks. This choice was justified when later on, the analysis showed their network properties were quite similar to those of domestic banks. Table (1)shows the market share in the banking sector of domestic banks and foreign bank branches as of end-September 2010.

Table 1: Assets by different types of institutions, end-September 2010

	Sep 2010 in local currency MM	%
Domestic Banks	95,255,691	81.16%
Foreign bank branches	22,106,349	18.84%
Total Banking system	117,362,039	100%

For these banks there were detailed information on interbank exposures disaggregated into 27 different asset classes as of end September 2010, as shown in Table 2. The different asset categories distinguish between:

- Overnight deposits (denominated in domestic and foreign currencies)
- Short-term deposits up to one year (denominated in domestic and foreign currencies)
- Repos (denominated in domestic and foreign currencies)

- Derivatives (denominated in domestic and foreign currencies)
- Interbank claims (denominated in domestic and foreign currencies)

Within these categories, there were additional subcategories corresponding to different maturities: overnight, less or equal to one year, or more than one year. The dataset, hence, consists of a three-dimensional matrix with dimensions $25 \times 25 \times 27$. In addition, we have the capital and levels and detailed balance sheet structures of all the institutions in the network shown in Table 2.

Figure 1 provides a graphical visualization of the banking network. A quick glance at it highlights how closely this network resembles a multi-money center network (Allen and Gale, 2000,[2]), that is, a network where a few banks, i.e. banks B1, B3, B5, B7, B9 and B10, have a central role connecting all the banks in the network. A couple of banks are just weakly connected to the network, i.e. B13 and B6, while one bank is completely disconnected (B24). While we analyze it formally later, the graphical evidence already suggests a network with a high degree of clustering.

Figure 1: Visualization of the network of an advanced emerging economy in Sep 2010: $n = 25$. number of links m= 350. Please note node size and distance are not of scale. Links are undirected.

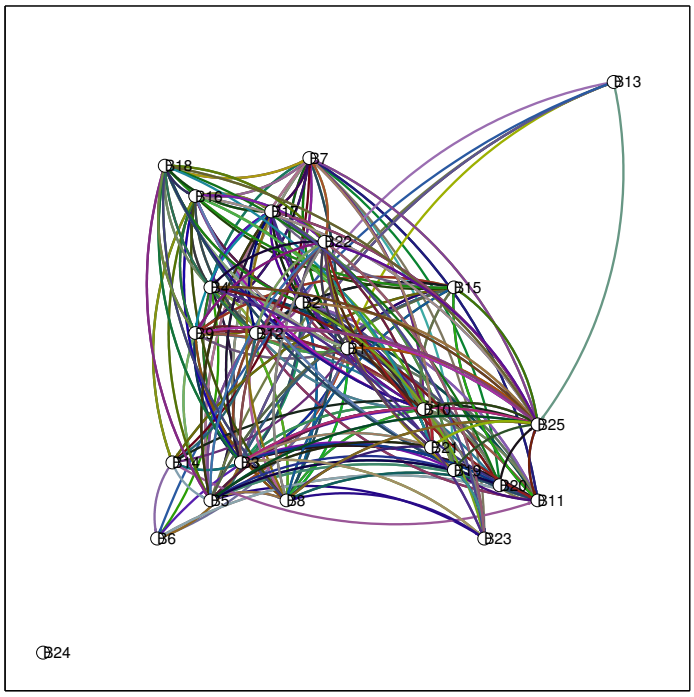

Table 3 on page 13 shows the banks' regulatory capital ratios, or equity to risk-weighted assets. All banks in our network exceed the minimum regulatory requirement of 8 percent proposed by the Basel Committee

Table 2: Asset classes, maturity and currency denomination

Exposure type	Maturity	Currency of denomination	Type of instruments
1	Overnight	Domestic, nominal	Checking accounts, other sight deposits, in-due process
2	Overnight	Domestic, UF denominated	
3	Overnight	Foreign currency	
4	Less or equal to a 1 year	Domestic, nominal	Term deposits, in-due-process
5	Less or equal to a 1 year	Domestic, UF denominated	Term deposits, in-due-process
6	Less or equal to a 1 year	Foreign currency	Term deposits, in-due-process
7	More than 1 year	Domestic, nominal	Term deposits, in-due-process
8	More than 1 year	Domestic, UF denominated	Term deposits, in-due-process
9	More than 1 year	Foreign currency	Term deposits, in-due-process
10	Over night	Domestic, nominal	Repos
11	Over night	Domestic, UF denominated	Repos
12	Over night	Foreign currency	Repos
13	Less or equal to 1 year	Domestic, nominal	Repos
14	Less or equal to 1 year	Domestic, UF denominated	Repos
15	Less or equal to 1 year	Foreign currency	Repos
16	Less or equal to 1 year	Domestic, nominal	Derivatives
17	Less or equal to 1 year	Domestic, UF denominated	Derivatives
18	Less or equal to 1 year	Foreign currency	Derivatives
19	More than 1 year	Domestic, nominal	Derivatives
20	More than 1 year	Domestic, UF denominated	Derivatives
21	More than 1 year	Foreign currency	Derivatives
22	Less or equal to 1 year	Domestic, nominal	Interbank claims
23	Less or equal to 1 year	Domestic, UF denominated	Interbank claims
24	Less or equal to 1 year	Foreign currency	Interbank claims
25	More than 1 year	Domestic, nominal	Interbank claims
26	More than 1 year	Domestic, UF denominated	Interbank claims
27	More than 1 year	Foreign currency	Interbank claims

(whereas investors typically favour 10% minimum). Government bonds, which carry a zero risk weight, comprise the larger share of assets held by the banks. Following Cont et al (2012) [20] we also report other useful size and several relative exposure (RE) measures. These measures include:

1. Total Capital (TC_i)= Tier 1 + Tier 2 Capital for bank i. E_i is the total exposure of bank i , essentially the total interbank liabilities of bank i in the network. TC = Core Capital + Provisions + Subordinated bonds + Minority Interest. Total Capital Ratio $TCR_i = {}^{TC_i}/_{RWA_i}$. RWA_i is the risk-weighted Assets of bank i.

2. Tier 1 Capital Ratio $T1CR_i = {}^{Tier\,1\,Capital_i}/_{RWA_i}$. Prudential regulations stipulate that this ratio exceeds the minimum regulatory capital requirement.

3. Basic Capital Ratio$BCR_i = {}^{Tier\,1\,Capital_i}/_{A(i)}$. $A(i)$ is the un-weighted assets of bank i.

4. The Cont et al (2012)[20] measures of relative exposure are: (1).$RE_i^1 = {}^{TC_i}/_{E_i}$ (2). $RE_i^2 = {}^{Tier1C_i}/_{max\,Ei,j}$. (3).$RE_i^3 = {}^{Tier1C_i}/_{E_i+RWA_i}$.

5. We calculate bank size as percent of assets in the whole banking network, as comparison. Please note B24 has no interbank exposure.

Conflicting conclusions can be drawn from observations: B12, 13 and 14 have very large TCR, and T1CR ratios. This is likely due to they hold large amount of government bonds as assets, which has a zero or low risk. Non-targeted capital ratios adopted by regulators (TCR, T1CR and BCR) do not show insufficient capital buffer in the banking network. However, relative exposure measure RE^1 show B3, 9, 12, 14 and 18 have relatively thin capital (<1), with the capital not enough to cover its total exposure. $RE^2(> 1)$ shows all banks have sufficient capital to cover its largest counterparty exposure. Using RE^3 as an alternative capital ratio to target high concentration nodes, there are quite a few nodes that have relatively thin capital ratio ($RE^3 < 10\%$), B1, 2, 3, 5, 7, 8, 16, 20 and 25. Among these nodes, B1, 3, 5, 10 are large in size ($Size\% > 10$), which account for almost 70% of the total assets.

3.2 Network Properties

3.2.1 Degrees of Connection

This section analyzes the topological characteristics of the banking network. An interbank network can be modeled as a weighted directed graph, defined as a triplet $I = (V, E, c)$,where:

- V is a set of financial institutions, each is denoted by number $n = 1, 2, 3, ...$
- E denotes a matrix that represents a bilateral exposure data between each pair of the counter-parties. $E_{i,j}$ represents the exposure of bank i on bank j, in other words, how much bank j owes bank i. It is the short term maximum loss of bank i caused by an exogenous default of bank j

Table 3: Capital and Relative Exposure Measures, end-September 2010. Critical values are highlighted: Blue highlights mean sufficient or large. Red highlights mean insufficient or small. We **bold font** the Domestic Banks (**DBs**), most of which are the core (nodes that have large connectivity and exposure) of the network shown in Figure 1 on page 10. Here, for simplicity, we define money centre with connectivity of 75 percentile or above. We denote the core with a star (*). Please note that some foreign bank branches that have strong presence in this economy also act like core, e.g. B4*. They are consistent in the paper, in Table 5 on page 17, Figure 6 on page 29 and 8 on page 31.

	TCR (%)	T1CR(%)	BCR (%)	RE_i^1	RE_i^2	RE_i^3(%)	Size(%)
B1*	13.64	8.79	6.72	5.6295	14.58	**8.58**	**17.45**
B2*	11.74	7.43	5.24	1.8454	6.39	**6.99**	**0.75**
B3*	11.85	8.01	4.8	**0.9941**	1.96	**7.16**	**16.50**
B4*	15.42	12.60	9.09	2.8797	10.02	11.96	4.73
B5*	13.64	9.38	7.01	4.4535	10.64	**9.10**	**12.24**
B6	**59.21**	**58.95**	**54.18**	**19.8519**	67.14	**57.25**	**0.03**
B7*	12.82	8.76	6.76	4.5874	14.58	**8.52**	6.46
B8	12.22	9.23	6.74	8.8715	24.03	**9.11**	2.77
B9	13.45	13.45	6.37	**0.4977**	2.52	10.59	1.25
B10*	14.52	10.50	7.2	5.2123	18.80	10.22	**20.80**
B11*	13.88	12.50	9.08	3.3736	6.38	12.01	3.23
B12	**126.39**	**126.39**	29.75	**0.7344**	3.41	**46.45**	**0.47**
B13	**124.36**	**124.36**	64.55	2.6744	5.46	**84.89**	**0.02**
B14	**115.79**	**115.79**	22.83	**0.7847**	4.32	**46.77**	**0.08**
B15	**88.91**	**88.78**	**37.97**	**3.6271**	11.65	**71.30**	**0.29**
B16*	12.96	8.77	6.22	2.2496	8.17	**8.29**	2.75
B17	19.37	14.08	10.27	1.9690	5.78	12.81	**0.83**
B18*	**28.9**	**28.90**	8.26	**0.4861**	2.98	18.12	**0.86**
B19	16.44	16.42	13.36	**76.4129**	86.48	16.38	**0.21**
B20	10.75	10.75	6.4	1.3462	3.18	**9.96**	**0.51**
B21	25.52	25.52	13.68	1.2815	3.14	21.28	**0.33**
B22	47.12	47.40	19.42	2.8666	9.16	**40.67**	**0.22**
B23	15.04	15.04	13.06	3.3545	13.06	14.40	**0.17**
B24	**192.43**	**192.43**	70.53	-	-	**192.43**	**0.16**
B25*	13.13	8.57	6.26	3.3710	9.54	**8.25**	6.88

Table 4: Summary of connectivity measures

Summary	$k_{in}(i)$	$k_{out}(i)$	$k(i)$	***A(i) MM$***	***L(i) MM$***
Mean	14	14	28	171500.65	171500.65
Standard deviation	7	6	12	281567.60	242075.25
Minimum	0	0	0	0.00	0.00
10th percentile	3	5	8	846.36	185.82
30th percentile	10	11	22	28043.90	8811.81
50th percentile	17	16	33	70042.82	85702.52
75th percentile	18	19	36	219226.28	234782.75
Maximum	23	22	45	1374956.94	929915.91

- c_n is the capital of each institution in the network, where $n = 1, 2, 3, ...$ Capital acts as the first buffer to absorb losses

In a directed graph, the *degree* of a node is defined as the number of edges directed towards or originated from a node. If the edge originates from a note it is counted as $out - degree$, K_{out}, if the edge is directed towards the node, it is counted as $in - degree$, K_{in}. For $i, j \in V$,

- $K_{in}(i) = \sum_{j \in V} \mathbf{1}_{E_{ij}>0}$ measures the number of institution i's debtors.
- $K_{out}(i) = \sum_{j \in V} \mathbf{1}_{E_{ji}>0}$ measures the number of institution i's creditors.
- The degree of connectivity is measured by $K_i = K_{in}(i) + K_{out}(i)$.
- The total interbank assets for institution i is denoted as $A(i) = \sum_{j \in V} E_{ij}$
- The total interbank liabilities for institution i is denoted as $L(i) = \sum_{j \in V} E_{ji}$

The summary statistics are presented in the table below.

3.2.2 Density, reciprocity, eccentricity and diameter

Density: The *connectivity* of a network, p, is the unconditional probability that two nodes share one link. *Density* refers to the ratio of the number of edges E to the number of possible edges. Suppose there are n nodes and m directed links, $p = \frac{m}{n(n-1)}$. $\frac{1}{n} \leq p \leq 1$. At its smallest value, $\frac{1}{n}$, the network is a tree shaped network. At its peak value, 1, the network is a complete network, meaning every node has interbank exposure in both directions (in and out) to every other node in the network. In our network, $n = 25$, $m = 350$, $density = \frac{m}{n(n-1)} = \frac{350}{25 \times 24} = 0.5833$. As a comparison, the smallest value of *density* in a network with the same number of nodes ($n = 25$) to out network is $density_{min} = \frac{1}{n} = \frac{1}{25} = 0.04$.

Reciprocity: *Reciprocity* refers to the *fraction* of links connecting the same two nodes in the network, and have both direction (in and out), which is denoted as r here. In our network, $r = \frac{89}{350} = 25.43\%$. This means about one quarter of the links are reciprocal. In other words, one quarter of the interbank exposure are bilateral among all the pairs of counter-parties.

Eccentricity: The *eccentricity* of node i represents the maximum distance to any other node in the network, is denoted as $\varepsilon_i = max_j d_{ij}$. In our network, since bank 24 is not accessible for all the other banks in the

network, the *eccentricity* of any bank i becomes ∞. However, if we ignore bank 24, the eccentricity of each bank i can be calculated (Table 9 on page 33). The *diameter* of a network is defined as $D = max_i \varepsilon_{ij}$. Similarly to eccentricity, since bank 24 is not accessible from other banks, D is ∞. However, if we ignore node 24, $D = 2$. The results are presented in Table 5.

3.2.3 Random graph or small-world?

Let n be the number of vertices in a graph and k be average edges of any vertex has. Note that in a regular ring lattice type of random graph with rewired probability $p \longrightarrow 0$, based on the same vertex set of our network (excluding B24), its *average path length* $L \sim \frac{n}{2k} \gg 1$, *and* $C \sim \frac{3}{4}$. *As* $p \longrightarrow 1$, *the* graph becomes a completely random rewired graph, with $L \approx L_{random} \approx \frac{ln(k)}{ln(n)}$, *and* $C \approx C_{random} \approx \frac{k}{n}$. In the two limiting cases, the regular lattice graph is a highly clustered, large world, with L grows linearly with n, whereas the random graph with $p = 1$ is a poorly clustered, small world, where L grows only logarithmically with n. The *small-world* phenomenon appears when p grows from 0 to 1, adding a few "short-cuts" between otherwise distant nodes shortens $L(p)$, while $C(p)$ remains high (Watts and Strogats, 1998) [51]). It is defined by $L(p) \gtrsim L_{random}$, but $C(p) > C_{random}$.

Distance The analysis of the network first requires calculating the *distance* from node i to node j, defined as $d_{i,j}$, which is the length of the shortest the path between two nodes. If there is a link directed from node i to node j, $d_{i,j} = 1$. Table 9 shows the shortest paths between all pairwise combinations of banks. Since the distance between most pair of banks is either 1 or 2, the banking network is well connected. Bank 24 is not accessible at all.

Average Path Length The *average path length* of node i within the network is defined as $l_i = {}^1/_{(n-1)} \sum_{j \neq i} d_{i,j}$. In this banking network, the average path length is Inf, as there is a disconnected bank, namely bank 24. However, if we form a sub network except for bank 24 (the disconnected vertex), the average path length for each vertex i, $\bar{L}_i$, can be calculated, as shown in Table 5. The average path length for our network, $\bar{L}$, is **1.3659**. This is slightly larger than $L_{random,n=25,k=14} = 1.2197$, and $L_{random,n=24,k=14}$ =1.2042. We calculate the results when n=24 (the sub-graph excluding B24) as a comparison.

Clustering Coefficient Classic graph theory refers *clustering coefficient* to the degree to which vertices in a graph cluster together, that is to concentrate in groups with a high density of links. Empirical research show that in most real-world complex networks such as genetic networks, social networks and internet, vertices tend to have higher clustering coefficients than in the random network of Erdős and Rényi (1959)[27] (Watts and Strogatz, 1998 [51]). There are several different measures of clustering coefficients:

Global Clustering Coefficient It measures the overall clustering effect in the network (see Luce and Perry (1949) [39] and Wasserman and Faust (1994) [50]). It is calculated as follows:

$$C_{global} = \frac{3 \times \text{number of triangles}}{\text{number of connected triplets of vertices}} = \frac{\text{number of closed triplets}}{\text{number of connected triplets of vertices}}$$

The *global clustering coefficient* result for our network (excluding node 24) is **0.5297.** This shows our network is higher clustered compared to the Austrian network analyzed by Boss et al. (2004) [12], which has $C_{global} = 0.12 \pm 0.01$ (mean and standard deviation across 10 datasets).

Local Clustering Coefficient (LC1) It is a local version of the above global clustering coefficient measure (Newman, 2003 [43]) and defined as follows: $C_i = \frac{\text{number of triangles connected to vertex i}}{\text{number of triples centered on vertex i}}$

Results are presented in Table 5 on the following page (LC1).

Local Clustering Coefficient (LC2) This is another measures of local clustering coefficient developed by Watts and Strogatz (1998) [51], which is calculated as follows: Suppose that a vertex i has k_i neighbours; then at most $k_i(k_{i-1})/2$ edges can exist between each pair of two neighbours in the network. In other words, that is when every neighbour of vertex i is connected to every other neighbour of vertex i. Let C_i denote the fraction of these maximum possible edges that actually exist. $\bar{C} = \frac{1}{n}\sum_{i=1}^{n} C_i$ as the average of C_i over all i.

Table 5 (LC2) presents the results for the local clustering coefficients. The average local clustering coefficient of our network is 0.8267 (except for bank 24). Including Bank 24, the average local clustering coefficient is 0.7936. This is significantly higher than if the graph is a random graph of the same vertex set $C_{random,n=25,k=14} = 0.56$, $C_{random,n=24,k=14} = 0.5833$.

Our network is indeed a *small world* network as defined in Watts and Strogats (1998) [51], due to its higher local clustering coefficients, and only slightly larger APL, compared to its corresponding random graph.

3.2.4 Centrality

Eigenvector centrality is measured as follows:

Consider a graph $G := (V, E)$ with $|V|$ number of vertices. let $A = (a_{v,t})$ be the adjacency matrix. If $a_{v,t} = 1$, vertex v is linked to vertex t, and $a_{v,t} = 0$ otherwise. The centrality score of vertex v can be defined as: $x_v = \frac{1}{\lambda}\sum_{t\in M(v)} x_t = \frac{1}{\lambda}\sum_{t\in G} a_{v,t}x_t$ where $M(v)$is a set of the neighbors of v and λ is a constant. This can be rearranged and rewritten in vector notation as the eigenvector equation $\mathbf{Ax} = \lambda\mathbf{x}$. Centrality measures the importance of nodes within a network. The result is presented in Table 5.

3.3 Distribution of connectivity measures

3.3.1 Parametric distribution fitting

Analyzing the distribution of connectivity and exposure further our understanding on interbank network structure. For K_{in} ,K_{out} , K and Exposure A we fit the following parametric distributions:

A. Lognormal distribution with mean $\mu$and standard deviation σ

pdf: $y = f(x|\mu,\, \sigma) = \frac{1}{x\sigma\sqrt{2\pi}} e^{\frac{-(ln\, x-\mu)^2}{2\sigma^2}}$

B. Extreme Value (EV) Distribution: location parameter μ and scale parameter σ;

pdf [1]: $y = f(x|\mu,\, \sigma) = \sigma^{-1}\, exp(\frac{x-\mu}{\sigma})\, exp(-exp(\frac{x-\mu}{\sigma}))$

C. Weibull Distribution: location parameter a and scale parameter b. Please note that if T has a Weibull distribution with parameters a and b, then $log(T)$ has an extreme value distribution with parameters $\mu = log(a)$ and $\sigma = 1/b$.

pdf: $y = f(x|a,\, b) = \frac{b}{a}(\frac{x}{a})^{b-1} e^{-(x/a)^b}$

D. Truncated Pareto distribution fitting, which is a semi-parametric fitting process, discussed in detail in the section 3.3.2

[1] This form of EV distribution is suitable to measure the minimum values of a distribution whose tail decays exponentially fast, such as normal distribution. To model the largest values, one may use the negative of the original values.

Table 5: Network Property Summary Table. Significant values are highlighted in red. Eccentricity (Ecc). Average Path Length (APL): Core money centres of the network (APL<1.20) include B1, 4, 5, 8, 10, 11, 25. The rest are peripheral nodes. Local clustering coefficients (LC1 and LC2). EC (Eigenvector Centrality) Ej,i (un)wgt is the importance of banks as debtors. EC Ei,j (un)wgt is the important of banks as creditors. "wgt" is weighted version that account for the weights of the flows of debts/credits. High concentration nodes are highlighted in red by a critical value of the 75 percentile of the series, which is 0.1394. B1, 3, 5, 7, 9, 10,12, 18 and 25 are large debtors; B1 3 5 10, 12 and 25 are large creditors.

	Ecc.	APL	LC1	LC2	EC Ej,i (unwgt)	EC Ei,j (unwgt)	EC Ej,i (wgt)	EC Ei,j (wgt)
B1*	2	**1.0435**	0.1696	0.6829	0.2567	0.2525	**0.1500**	**0.3400**
B2*	2	1.2174	0.205	0.8307	0.2353	0.2317	0.0225	0.0173
B3*	1	1	0.154	0.6167	0.2638	0.2641	**0.2699**	**0.7799**
B4*	2	**1.1739**	0.2112	0.8055	0.2341	0.2159	0.0630	0.1241
B5*	2	**1.1304**	0.1795	0.7323	0.2528	0.2523	**0.5267**	**0.2058**
B6	2	1.8261	0.0972	0.7353	0.0353	0.0738	0.0002	0.0010
B7*	2	1.2609	0.1857	0.8127	0.2287	0.2437	**0.2177**	0.1131
B8	2	**1.1304**	0.2472	0.8947	0.2437	0.2113	0.0594	0.0240
B9	2	1.2174	0.2268	0.9127	0.2283	0.2173	**0.1696**	0.1284
B10*	2	**1.1304**	0.1776	0.7372	0.2526	0.2525	**0.5875**	**0.3069**
B11*	2	**1.1739**	0.2095	0.7850	0.2410	0.2215	0.0549	0.0687
B12	2	1.2609	0.2379	0.9064	0.2307	0.2113	**0.2439**	**0.1726**
B13	2	1.913	0.0238	0.8250	0.0316	0.0650	0.0000	0.0017
B14	2	1.8696	0.0321	0.8333	0.0410	0.1322	0.0000	0.0103
B15	2	1.4348	0.2482	0.8792	0.1777	0.1518	0.0147	0.0192
B16*	2	1.2609	0.1849	0.8157	0.2287	0.2480	0.0773	0.0678
B17	2	1.4348	0.129	0.8075	0.1733	0.2465	0.0065	0.0343
B18*	2	1.2174	0.2317	0.8881	0.2435	0.2255	**0.1563**	0.1079
B19	2	1.6087	0.3516	0.8864	0.1203	0.0686	0.0007	0.0004
B20	2	1.6522	0.1333	1	0.1198	0.1042	0.0075	0.0330
B21	2	1.5652	0.1759	0.9835	0.1444	0.1905	0.0087	0.0435
B22	2	1.3043	0.1989	0.848	0.2199	0.2235	0.0090	0.0132
B23	1	1	0.2316	0.8462	0.1225	0.1049	0.0001	0.0017
B24	Inf	-	-	0	0	0	0	0
B25*	2	**1.1304**	0.1956	0.7741	0.2477	0.2404	**0.3233**	**0.1965**
mean(ex. B24)	1.9167	1.3315	0.1849	0.8266	-	-	-	-
mean (inc. B24)	Inf	-	-	0.7936	-	-	-	-

E. Normal-Laplace (N-L) and Double Pareto Lognormal (dPlN) Distributions, discussed in detail in the Appendix.

Figure 2 shows the fitted distributions with the empirical pdf, while the estimated parameters are presented in Table 6. The data suggests, as evident by the titling point in the plots reported in Figure on page 22 that the dPlN distribution best fit the data. This distribution falls somewhere in between lognormal and Pareto distribution (see Reed and Jorgensen, 2004, [45] and the statistical appendix). Our choice of the dPlN distribution is inspired by the core-peripheral network structure displayed in Figure 1, suggesting possible two tail in both ends of the connectivity and exposure distributions. This distribution was first discovered by Mitzenmacher (2001) that "have a lognormal body and Pareto tail" (Reed and Jorgensen, 2004) [45].

Equation 31 on page 36 and Equation 32 on page 36 show the limiting cases for the paretian tail indices when the distribution approaches right (∞) and left (0), respectively. The results of our network distribution are presented in Table 6d on page 20. We can view these results as the paretian tail index estimates in the limiting cases (should the network expands), and they are comparable to the results presented in the truncated Pareto case in Section 3.3.2 on page 21. This is an evidence of possible community structure and hierarchy within our network.

Figure 2: Fitted lognormal v.s. empirical pdf of $k_{in}(i)$,$k_{out}(i)$, $k(i)$ and Exposure A $(in\, 10^{10}\, local\, currency)$

(a) K_{in}

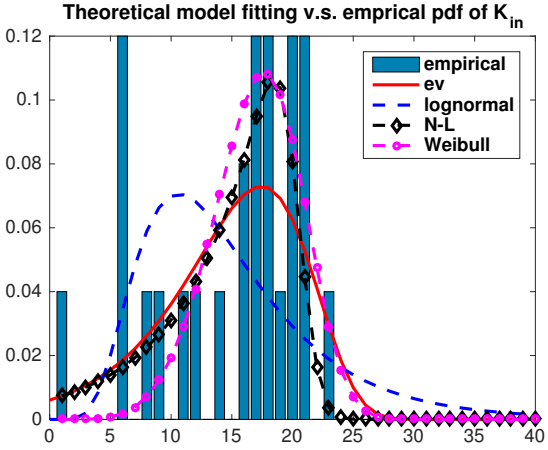

(b) K_{out}

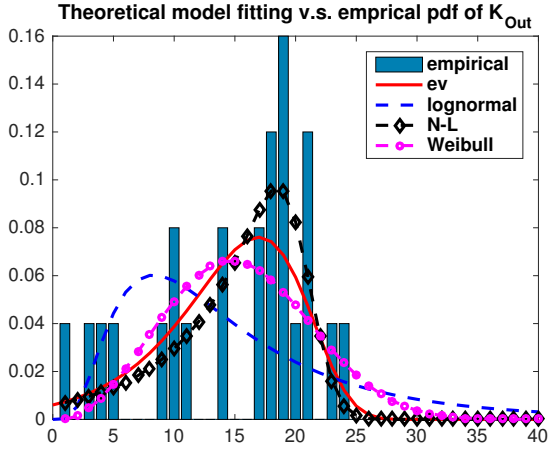

(c) K

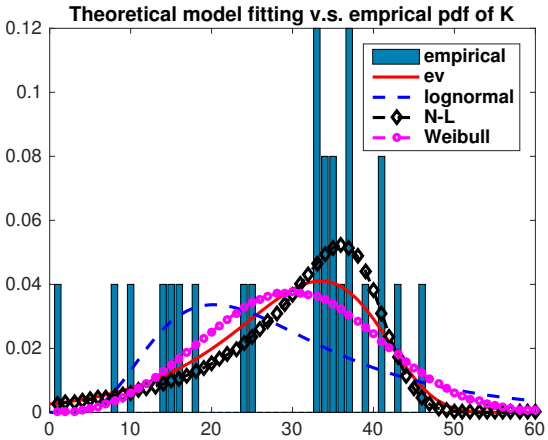

(d) A

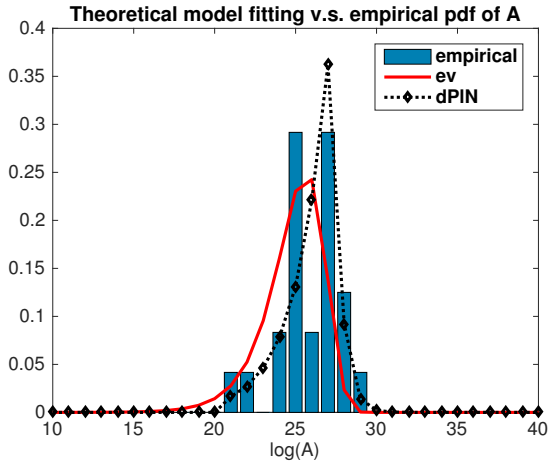

Table 6: Distribution parameter estimates of K_{in}, K_{out}, K and exposure A_i (*in 10^{10} of domestic currency). CI refers to confidence intervals. nll refers to negative log-likelihood. The returned value of $AD\,h = 0$ is the hypothesis test result, which indicates that Anderson-Darling test fails to reject the null hypothesis of the respective assumption of distributions at the default 5% significance level, and vice versa. cv refers to AD critical values.

(a) Log-normal distribution fitting: As expected at 5% significant level, A-D test reject the hypothesis of lognormal distribution for K_{in} , K_{out} , K and A.

	μ	$CI_{\alpha=5\%}$	σ	$CI_{\alpha=5\%}$	nll	AD h	$p_{\,AD,\,5\%}$	AD statistics	cv
K_{in}	2.7298	[2.5894, 2.8702]	0.3084	[0.2360, 0.4453]	61.9218	1	0.009	1.0073	0.7553
K_{out}	2.5354	[2.2622, 2.8085]	0.6469	[0.5028, 0.9075]	83.9508	1	0.0092	1.0131	0.7273
K	3.2712	[3.0547, 3.4879]	0.5129	[0.3986, 0.7195]	96.0405	1	0.0037	1.1668	0.7262
A	24.7964	[23.9938, 25.599]	1.9007	[1.4772, 2.6662]	644.0808	1	0.0000	2.8928	0.7262

(b) Weibull distribution fitting: The A-D test shows strong evidence to reject the null hypothesis of Weibull distribution in the case of K_{in} , K_{out} , K. However, fail to reject the hypothesis of Weibull distribution in the case of Exposure A. We further tests goodness-of-fit of the extreme value distribution to the distribution of log(A) in tab 6c.

	a	$CI_{\alpha=5\%}$	b	$CI_{\alpha=5\%}$	nll	AD h	$p_{\,AD,\,5\%}$	AD stat	cv
K_{in}	17.4285	[15.9514, 19.0424]	5.0391	[3.5145, 7.2250]	57.9402	1	0.0026	1.2296	0.7387
K_{out}	16.2917	[13.9821, 18.9827]	2.71171	[1.9056, 3.8589]	77.5211	1	0.0013	1.3490	0.7393
K	32.6124	[28.5729, 37.2229]	3.1478	[2.2181, 4.4671]	91.1131	1	0.0000	1.4109	0.7387
A	13.6895*	[7.3731*, 25.4171*]	0.6807	[0.4989, 0.9288]	642.1669	0	0.7832	0.2440	0.7387

(c) Extreme value distribution fitting: The A-D test does not reject the null hypothesis of extreme value distribution with moderate evidence (p-value at 5%) in the cases of K_{in} , K_{out} , K, whereas, it rejects the null hypothesis in the case of Exposure A, with strong evidence. For the distribution of log(A), A-D test shows no evidence of rejection. Together with evidence shown in sub-table 6b, it is intuitive that this specific class of extreme value distribution fits well with the logarithmic form of the exposure distribution, and the distributions of in and out-degree and connectivity.

	μ	$CI_{\alpha=5\%}$	σ	$CI_{\alpha=5\%}$	nll	AD h	$p_{\,AD,\,5\%}$	AD stat	cv
K_{in}	16.662	[14.883 18.441]	4.3245	[3.1260 5.9827]	76.9965	0	0.1163	0.5984	0.7393
K_{out}	16.9521	[14.9619, 18.9422]	4.8353	[3.5034, 6.6735]	79.6616	0	0.1172	0.5972	0.7393
K	33.4891	[29.8050, 37.1733]	8.9545	[6.4834, 12.3676]	95.1290	0	0.0511	0.7358	0.7393
A	34.3361*	[15.2187*, 53.4534*]	45.6317*	[35.9967*, 57.8456*]	705.5769	1	0.0000	4.8015	0.7393
$log(A)$	25.6425	[25.0237, 26.2613]	1.4691	[1.0767, 2.0044]	47.0536	0	0.7832	0.2440	0.7387

(d) N-L and dPlN distributions fitting using MLE. Please note that, as we understand, and evidences shown in sub-table 6b and 6c, we are fitting distribuiton of in and out-degree and connectivity to Normal-Laplace distribution, and we are fitting Exposure to Double Pareto Log-normal distribution. Please note that dPlN is the exponential form of the N-L distribution.

	α	β	ν	τ	nlog-likelihood
K_{in} **(NL)**	3.9189	0.1604	20.1082	1.3260	457.3975
K_{out} **(NL)**	2.9628	0.1604	20.4802	1.7901	273.0211
K **(NL)**	1.1735	0.0887	39.5836	3.3891	235.0851
A (dPlN)	1.8732	0.5210	26.1820	0.1651	1.6204e+03

3.3.2 Semi-parametric heavy-tail distribution fitting

The failure to fit a lognormal distribution to the connectivity measures steers the analysis towards the detection of heavy tails, or the so-called *scale-free* property, which can be assessed from an analysis of log-log plots of the complementary cumulative distribution function (CCDF), which is simply given by $\mathbb{P}(K_{out} \geq k)$, $\mathbb{P}(K_{in} \geq k)$, $\mathbb{P}(K \geq k)$ and $\mathbb{P}(A \geq a)$ for the out-degree, in-degree, degrees of connectivity and exposure respectively. The *scale-free* property occurs quite often in nature, i.e. earthquake intensity, and man-made phenomena, i.e. city population, income distribution, etc. Many known large complex networks such as internet, actors collaboration, genetic networks, exhibit *scale-free,* or *power-law* distribution in their connectivity. This is due to two generic characteristics: (i) networks expand continuously as new vertices enter the system, and (ii) new vertices have *preferential attachment*s [6]). In interbank networks the *scale-free* property is present in the Austrian and Brazilian networks (see Boss et al. (2004) [12] and Cont et al. (2012) [20]). *Preferential attachments* in interbank network refers to the phenomenon that new banks entering the network tend to connect to banks that already have more links to other neighbours. In a *scale-free* network, the first two moments of the distribution, the mean and standard deviation, are not enough to represent the empirical distribution of the data since the density of the distribution is heavily weighed in the right tail, as implied by the *power-law* distribution: $p(x) \sim x^{-\alpha}$, where α is the *exponent* or *scaling* parameter. Normally, $2 < \alpha < 3$, with some exceptions. The analysis of empirical data sets finds that above a minimum threshold value, x_{min}, the *tail* of the distribution follows a *power-law* (Choromanski et al., 2013 [18]; Onnela et al., 2007[44]).

Detecting heavy tails and estimating the parameters of a power law distribution is relatively difficult. Traditional least squared fitting, developed by Pareto's work in 19th century (Arnold, 1983 [5]), can produce inaccurate results. Clauset et al (2009) [19] have suggested combining maximum likelihood estimation (MLE) with goodness-of-fit tests such as Kolmogorov-Smirnov (K-S) statistic and likelihood ratios.

We follow Clauset et al. (2009) [19] in our analysis, and use MLS with K-S Statistics, with adjustment to finite sample. Table 7 shows the key statistics, and Figure 3 shows the log-log plots of the CCDF of K_{in},K_{out},K and exposures$A$, and the corresponding fitted power law distribution. According to Clauset et al. (2009) [19], when the sample size $n \lesssim 100$, and p-values for the tested distributions are above our threshold of **0.1**, the power-law hypothesis cannot be ruled out. Our sample size, however, is very small which makes difficult for the test to single out the true power-law distribution from others, e.g. exponential, lognormal etc. This problem disappears as the sample size increases since the p-values for the non-power-law distributions drop off. Hence, even if the data set is sampled from a power law distribution, the small data sample prevents a good fit, which is evident by the large standard deviations of the parameter estimates in Table 7.Nonetheless, the clear and distinct double tail features shown in Figure 3, exhibit two regions in connectivity and exposure measures that could be fitted with power. Overall, the tail indices in our interbank network where prominent with statistical significance (K-S test p value $>$ **0.1***).

Table 7: Key Statistics of MLE and K-S for $K_{in}(i)$,$K_{out}(i)$, $K(i)$ and$A(i)$ (**in 10^8 local currency). Data is for Sep 2010. This table is accompanying Figure 3. $k_{in,\,min}$, $k_{out,\,min}$, k_{min} are selected by the fitted distributions that have the minimum of K-S goodness-of-fit statistics (D). We use the hatted parameters for estimation of the (unhatted) true (unobserved) variables; subscript 1 and 2 denote left and right tail statistics respectively: $\hat{\alpha}_1$ and $\hat{\alpha}_2$ are the estimated left and right tail indices, $\hat{\sigma}(\hat{\alpha}_1)$ and $\hat{\alpha}_2$ are the estimated standard deviation of $\hat{\alpha}_1$ and $\hat{\alpha}_2$. This is equivalent to the Hill (1975) [34] estimator. $Limit_1$ is the upper limit of the data analysed as this is a truncated Pareto distribution (selected based on observation of Figure 3), and it is only defined for the left tail in this test. The right tail is the natural upper limit of the entire distribution. L_1 and L_2 are the log-likelihood estimates for left tail and right tail distribution. p_1 and p_2 are the p-values of K-S test (when larger than **0.1** - significant*). Large $\hat{\alpha}$ and $\hat{\sigma}(\hat{\alpha})$ may be caused by the small sample bias. Further data will be collected to verify the test results.

Left tail statistics					Right tail statistics				
	$k_{in}(i)$	$k_{out}(i)$	$k(i)$	A_i^{**}		$k_{in}(i)$	$k_{out}(i)$	$k(i)$	A_i^{**}
$\hat{\alpha}_1$	1.4792	1.1917	1.2875	1.1949	$\hat{\alpha}_2$	4.7500	4.7333	4.7500	2.5421
$\hat{\sigma}(\hat{\alpha}_1)$	0.3038	0.6825	0.6685	1.1554	$\hat{\sigma}(\hat{\alpha}_2)$	0.6787	0.6542	0.6744	1.1813
$\hat{k}_{in,min\,1}$	5	2	7	4**	$\hat{k}_{in,min\,2}$	15	16	32	1630.1722
$Limit_1$	12	15	30	1630.1722**	$Limit_2$	-	-	-	-
L_1	-92.2793	-110.2908	-110.5894	-215.2695	L_2	-58.4769	-45.9618	-44.0562	-61.4525
p_1	**0.7430***	**0.2150***	**0.3030***	0.0000	p_2	0.002	0.007	0.0660	**0.9430***
D_1	0.4479	0.5791	0.3189	0.3646	D_2	0.1882	0.1940	0.2423	0.1005

Figure 3: Log log plot of ccdf of in-degree, out-degree and degree of connectivity and exposure in Sep 2010

(a) K_{in}

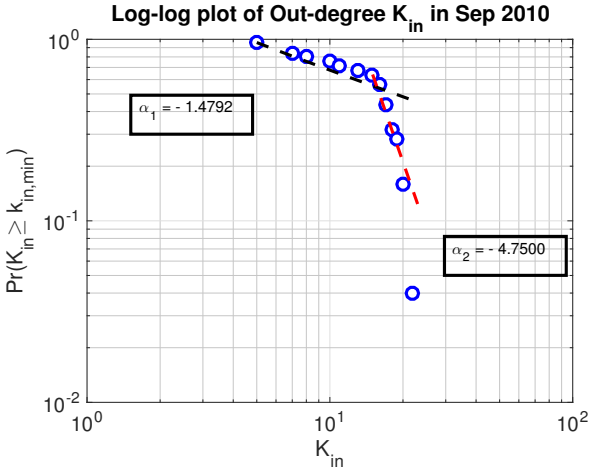

(b) K_{out}

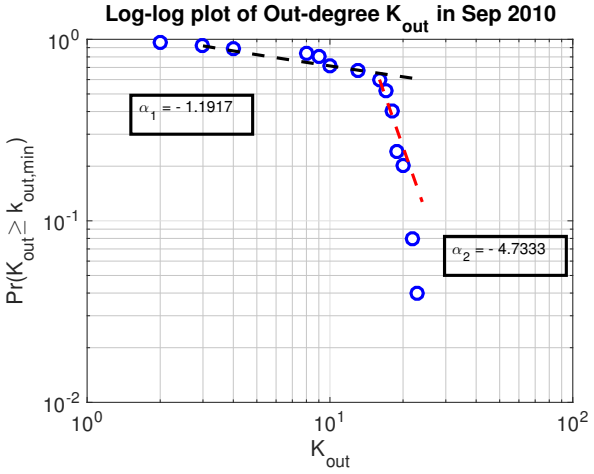

(c) K

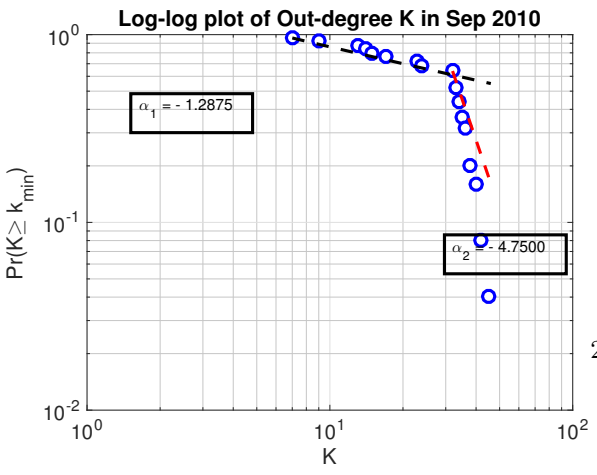

(d) Exposure (A)

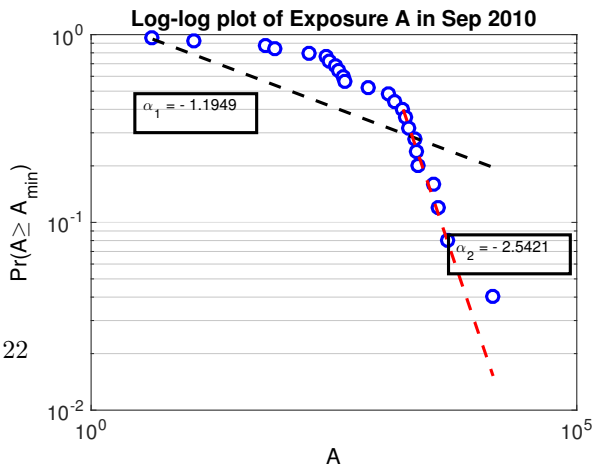

4 Systemic Risk Analysis in a Balance-Sheet Framework

While an examination of the topological properties of the interbank network is useful to determine the degree of interconnectedness among banks, and to make qualitative inferences about systemic risk, it is not enough to quantify systemic risk. Henceforth, we shift the focus to the analysis of systemic risk within a balance-sheet network framework, which can capture how connectivity affects the transmission of defaults within the network.

4.1 Default mechanism

A default event occurs when a bank is unable to fulfill its financial obligation, i.e. failure to repay principal or interests on contractual obligations, or inability to provide a scheduled loan as agreed with a counter-party. In theory, a institution fails when it becomes insolvent, i.e. its capital buffer is wiped out by credit and/or market losses. These losses can be triggered by exogenous events or macroeconomic shocks affecting the institution's earnings.

Prompt corrective action frameworks, however, suggest that insolvency may not be the most appropriate default event as regulatory intervention may occur prior to insolvency (Chan-Lau and Sy, 2007 [17]). For practical purposes, therefore, the default event is better defined as the point when the capital reserves of a bank fall below a minimum requirement established by the regulatory authority. For simplicity, we define a default event as the institute's failure to meet an arbitrary minimum capital requirement of 7 percent in our model. .

The balance-sheet network analysis follows Jo (2012) [35], which expands on Chan-Lau (2010) [15]. Conceptually, given the balance sheet of banks in the network at a given point in time, including interbank exposures, it subjects banks to credit losses and funding losses driven by the pre-specified default of one bank (or set of banks). Cash outflows and funding losses are linked to the solvency of the financial institution, representing liquidity and solvency risk.

The default simulation, illustrated in Figure 4c runs as the following steps:

- A set of defaulted institutions is defined as follows: $D = \{i : C_i - L_i < C_i^r(1 + b_i)\}$. where C_i is the capital held by the institution i, L_i is the institution's loss, C_i^rminimum threshold of capital required by regulator for institution i, and b_i is an additional capital buffer.

- Credit loss arises with counter-party defaults: Losses from claims on the defaulted institutions. In the case of a default by institution h, the exposure from institution i to$h$ can be expressed as E_{ih}. With the defined defaulted set of D, the credit loss ($CL_i = \sum_{h \in D} E_{ih}\delta$), where the *loss given default (LGD)*, δ is computed through exogenous default mechanism by Chan-Lau (2010) [15].

- Funding losses are calculated through a complex mechanism: To repay claims from defaulted (creditor) institutions, debtor institutions must be able to refinance through two sources: (1) sell part of its assets, or (2) get fundings from other alternative creditors. Under normal market condition, the troubled

Figure 4: Replacement rate and incremental funding cost rate

(a) replacement rate

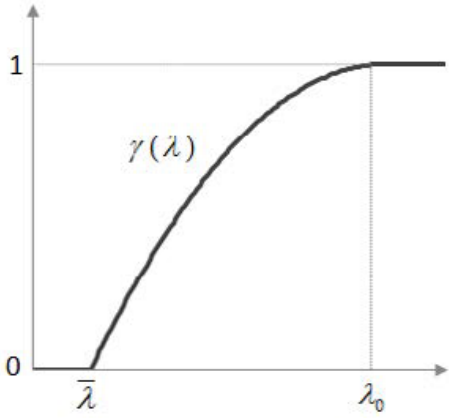

(b) Incremental funding cost loss ratio

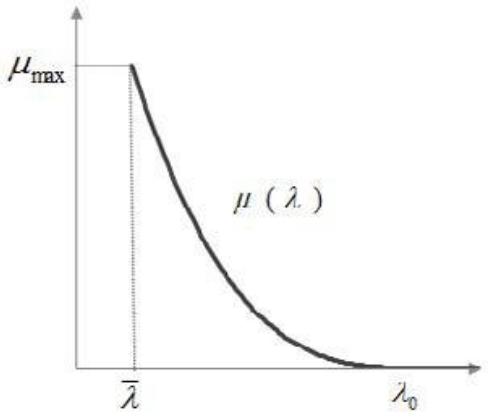

(c) Default contagion mechanism. CRRW (Capital ratio risk weighted)

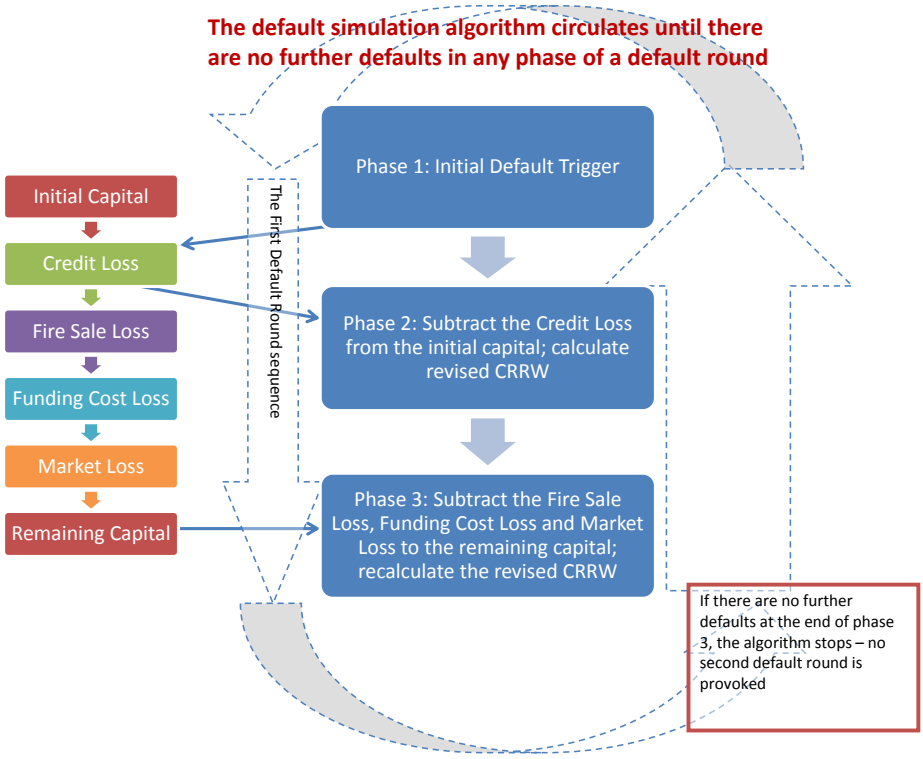

institution can sell its liquid assets at market price and can find alternative creditors easily. However, under stress scenarios, the troubled institution would have to sell its assets at fire sale prices and/or pay considerable additional funding costs to seek refinance. The funding losses are computed as follows:

1. After initial defaults, from defaulted set defined by D, institution i (as a creditor of the defaulted set D) would collect $\sum_{h\in D} E_{hi}$ from D. This amount is assumed to be withdrawn completely.

2. Institution i then replaces a part of cash outflow with funds newly borrowed from alternative creditors, and the replacement amount can be expressed by $\gamma \sum_{h\in D} E_{hi}$ $(0 \leq \gamma \leq 1)$, where γ is the replacement rate.

3. The difference between fire-sale prices and book values would induce losses for institution i. This is calculated by the price of liquid assets and illiquid assets and their loss rates. Let q denote fire-sale loss rate for liquid assets, and z define loss rate for illiquid assets[2]. Cash generated from fire-sales of liquid assets a_i^q is $a_i^q(1-q)$.

   (a) If the cash outflow can be covered by selling liquid assets, no illiquid assets are to be sold. Such condition can be written as $(1-\gamma)\sum_{h\in D} E_{hi} \leq a_i^q(1-q)$, institution i would sell a part of its liquid asset equivalent to the amount of $(1-\gamma)\sum_{h\in D} E_{hi}/(1-q)$, then it would take a loss of $(1-\gamma)\sum_{h\in D} E_{hi} \times {}^{q}/_{(1-q)}$. *The fire sale losses (FSL_i)* can be written as:

$$FSL_i = Min\left[(1-\gamma)\sum_{h\in D} E_{hi},\ a_i^q(1-q)\right] \cdot \frac{q}{1-q} \tag{1}$$

   (b) If the cash outflow cannot be recovered by selling illiquid assets, $(1-\gamma)\sum_{h\in D} E_{hi} > a_i^q(1-q)$, then institution i has to sell illiquid assets[3]. *The fire sale losses (FSL_i)* can be written as:

$$FSL_i = Min\left[(1-\gamma)\sum_{h\in D} E_{hi},\ a_i^q(1-q)\right] \cdot \frac{q}{1-q} + Max\left[(1-\gamma)\sum_{h\in D} E_{hi} - a_i^q(1-q),\ 0\right] \cdot \frac{z}{1-z} \tag{2}$$

4. Except for *fire sale losses,* an increase in funding costs can cause funding losses during the refinancing process for institution *i*. Jo (2012) [35] assumes that short-term debts are from two sources: (1) from the defaulted institutions, and the amount can be expressed as $\gamma \sum_{h\in D} E_{hi}$; (2) from the non-defaulted institutions, which can be written as $\sum_{k\notin D} E_{ki}^S$. Short term debts are considered extensively here because the more an institution replies on them, the more chances it would be subject to liquidity risk. Hence the *funding cost loss (FCL_i)* can be written as

$$FCL_i = \sum_{h\in D} E_{hi}\gamma\mu + \sum_{k\notin D} E_{ki}^S\mu \tag{3}$$

5. Calibration of the *replacement rate* γ*:* The replacement rate first declines as the capital ratio falls. It is assumed that there is a normal capital ratio λ_0 that an institution can completely rollover or find alternative creditors but below the regulatory capital ratio $\bar{\lambda}$ refinancing is not possible. This relationship can be expressed in mathematical form as below:

$$\gamma(\lambda) = \begin{cases} 1 & if\ \lambda_0 < \lambda \\ 1 - \frac{(\lambda_0-\lambda)^2}{(\lambda_0-\bar{\lambda})^2} & if \quad \bar{\lambda} < \lambda \leq \lambda_0 \\ 0 & otherwise \end{cases} \tag{4}$$

   This is illustrated in Figure 5.1 (a).

[2]It is reasonable to assume $q < z$

[3]It is reasonable to assume that illiquid assets should be sold only after all liquid assets are sold.

6. Calibration of funding cost loss ratio: An incremental funding cost adversely increases as the capital ratio falls. In the normal state (λ_0), replacement is not difficult to find at normal costs, so μ is set to zero. As a general rule, it is intuitive to link funding cost to relevant credit spread. Using empirical evidence between funding cost and solvency ability, a panel regression is fitted between credit spreads and capital ratios. The results by Jo(2012) [35] for Korea suggest that the credit spread is proportional to the third power of a decline in the capital ratio[4]. This relationship can be written in the mathematical formula as below:

$$\mu = \begin{cases} 0 & if\ \lambda_0 < \lambda \\ a \cdot (\lambda_0 - \lambda)^3 & if\ \bar{\lambda} < \lambda \leq \lambda_0 \end{cases} \tag{5}$$

where a is the proportional constant obtained by the regression. In our emerging market economy, this is relatively small, less than 1%. The upper bound of μ and γ are forecasted value at the regulatory capital ratio ($\bar{\lambda}$). See Figure 5.1.(b).

7. By combining 2, 3, 4, and 5, we can write the total *funding loss* as below:

$$\begin{aligned} FL_i &= FSL_i + FCL_i \\ &= Min\left[(1-\gamma(\lambda)) \sum_{h\in D} E_{hi},\, a_i^q(1-q)\right]\frac{q}{1-q} + Max\left[(1-\gamma(\lambda)) \sum_{h\in D} E_{hi} - a_i^q(1-q),\, 0\right]\frac{z}{1-z} \\ &\quad + \sum_{h\in D} E_{hi}\gamma(\lambda)\mu(\lambda) + \sum_{h\notin D} E_{ki}^S \mu(\lambda) \end{aligned} \tag{6}$$

4.2 Default simulation results (exogenous case)

4.2.1 Parameter calibration

The funding cost loss function needs to be calibrated according to each economy's funding characteristics. In Jo (2012) [35], the calibration results are based on data before Lehman bankruptcy (2007Q3 to 2010 Q3), and the regression is fitted as follows:

$$spread_t = 0.04 \times (14.62 - Basel\, ratio_t)^3 + 0.5 \tag{7}$$

The incremental funding cost function is estimated as$\mu(\lambda) = 0.04(14.62 - \lambda)^3$. The relationship between the capital ratio and bank bond spread is presented in 5.

For the advanced emerging economy analyzed here, there is limited data for calibrating the incremental funding cost function. We estimated a panel regression using July 2013 data of option-adjusted spreads (OAS) for eight institutions and the government yield curve as the risk-free rate to estimate the equation:

$$\mu = \begin{cases} 0 & if\ \lambda_0 < \lambda \\ a \cdot (\lambda_0 - \lambda)^r & if\ \bar{\lambda} < \lambda \leq \lambda_0 \end{cases}$$

where $\lambda_{0,\,i}$ is calculated as the historical average capital ratio before the crisis for each institution i. We found the following incremental funding cost loss equation in our market is $\mu = 0.0006495 \times (\lambda_0 - \lambda)^3$, which was used in the analysis of default contagion.

We also make the following assumptions, which are suggested by previous literature (Jo (2012) [35] and several others).

- The the fire sale loss rate for liquid assets:$q = 0.2$
- The fire sale loss rate for illiquid assets: $z = 0.7$

[4]This can be re-calibrated to fit each country's specific market characteristics.

Figure 5: Scatter plot between capital ratio and bank bond spread and out of sample forecast (Jo, 2012)

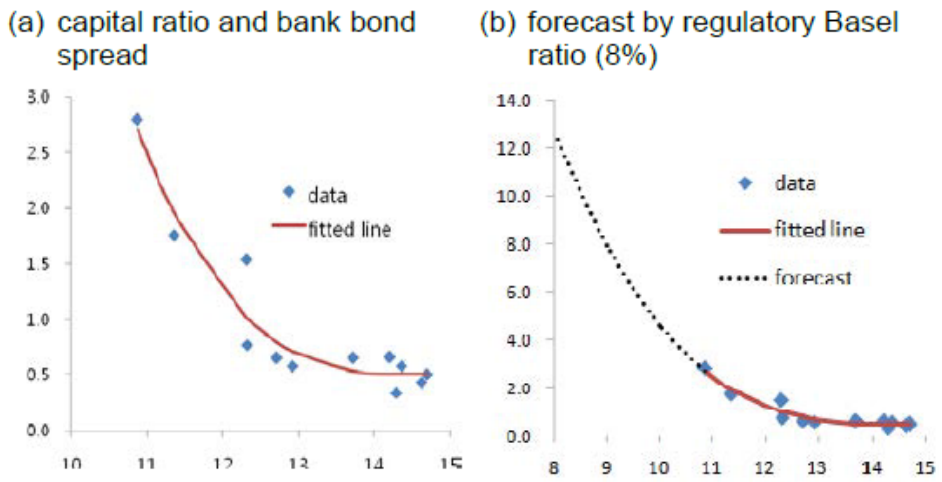

- Fair Value loss rate $FVLR = 0.2$.

Discussion: The results of the default simulations are summarized in Table 8 on the following page and Figure 6, 7 and 8 on page 31.

1. Using simulation analysis, any one single bank's default does not cause contagion due to direct counterparty exposure in the first round of the simulation. Majority of the damage is caused by fire-sales of assets and liquidity shortage. These in turn, would trigger second round default of several institutes with thin capital buffers, and so on and so forth. We assume multiple rounds of default simulations take place simultaneously.

2. Small banks by size (Table 3 on page 13) default may cause domino effects as much as larger banks' defaults, due to fire-sale of assets and liquidity shortage in the stress scenario, especially some small banks have large interbank exposures (see point 5).

3. By examining capital adequacy regarding bilateral exposures, relative exposure RE^3 in Table 3 shows B1, 2, 3, 4* 5, 7, 8, 9* 10*, 11*, 16, 17* 20, 25 (*banks at borderlines) are the ones with the thin capital buffer ($RE^3 < 10\%$).

4. Results from the default simulation (Table 8 on the next page and Figure 6, 7 and 8) show similar results to the relative exposure measure: The first round default due to secondary effect (fire-sale and funding loss in stress market conditions) are consistent: Bank 2, 3, 8, 9, 16, 18, 20, 21, and 25. The second round defaulted banks due to secondary effect are also consistent: 1, 5, 7, 10, 11, 22, with

Table 8: Default simulation result (exogenous case). Credit Shock (CS), Funding Shock (FS). Results show Direct counter-party exposure do not cause as much damage as Funding (liquidity) shock.

	Default round 1		Default round 2		Default round 3	
Initial trigger	CS	FS	CS	FS	CS	FS
Bank 1	n/a	2, 3, 8, 9, 16, 18, 20, 21, 25	n/a	5, 7, 10, 11, 22	4, 14	n/a
Bank 2	n/a	3, 8, 9, 16, 18, 20, 21, 25	n/a	1, 5, 7, 10, 11, 22	4, 14	n/a
Bank 3	n/a	2, 8, 9, 16, 18, 20, 21, 25	n/a	1, 5, 7, 10, 11, 22	4, 14	n/a
Bank 4	n/a	2, 3, 8, 9, 16, 18, 20, 21, 25	n/a	1, 5, 7, 10, 11, 22	14, 17	n/a
Bank 5	n/a	2, 3, 8, 9, 16, 18, 20, 21, 25	n/a	1, 7, 10, 11, 22	4, 14	n/a
Bank 6	n/a	2, 3, 8, 9, 16, 18, 20, 21, 25	n/a	1, 5, 7, 10, 11, 22	4, 14	n/a
Bank 7	n/a	2, 3, 8, 9, 16, 18, 20, 21, 25	n/a	1, 5, 10, 11, 14, 22	4	n/a
Bank 8	n/a	2, 3, 9, 16, 18, 20, 21, 25	n/a	1, 5, 7, 10, 11, 22	4, 14	n/a
Bank 9	n/a	2, 3, 8, 16, 18, 20, 21, 25	n/a	1, 5, 7, 10, 11, 22	4, 14	n/a
Bank 10	n/a	2, 3, 8, 9, 16, 18, 20, 21, 25	n/a	1, 5, 7, 11, 22	4, 14	n/a
Bank 11	n/a	2, 3, 8, 9, 16, 18, 20, 21, 25	n/a	1, 5, 7, 10, 14, 22	4	n/a
Bank 12	n/a	2, 3, 8, 9, 16, 18, 20, 21, 25	n/a	1, 5, 7, 10, 11, 14, 22	4	n/a
Bank 13	n/a	2, 3, 8, 9, 16, 18, 20, 21, 25	n/a	1, 5, 7, 10, 11, 22	4, 14	n/a
Bank 14	n/a	2, 3, 8, 9, 16, 18, 20, 21, 25	n/a	1, 5, 7, 10, 11, 22	4	n/a
Bank 15	n/a	2, 3, 8, 9, 16, 18, 20, 21, 25	n/a	1, 5, 7, 10, 11, 22	4, 14	n/a
Bank 16	n/a	2, 3, 8, 9, 18, 20, 21, 25	n/a	1, 5, 7, 10, 11, 22	4, 14	n/a
Bank 17	n/a	2, 3, 8, 9, 16, 18, 20, 21, 25	n/a	1, 5, 7, 10, 11, 22	4, 14	n/a
Bank 18	n/a	2, 3, 8, 9, 16, 20, 21, 25	n/a	1, 5, 7, 10, 11, 22	4, 14	n/a
Bank 19	n/a	2, 3, 8, 9, 16, 18, 20, 21, 25	n/a	1, 5, 7, 10, 11, 22	4, 14	n/a
Bank 20	n/a	2, 3, 8, 9, 16, 18, 21, 25	n/a	1, 5, 7, 10, 11, 22	4, 14	n/a
Bank 21	n/a	2, 3, 8, 9, 16, 18, 20, 25	n/a	1, 5, 7, 10, 11, 22	4, 14	n/a
Bank 22	n/a	2, 3, 8, 9, 16, 18, 20, 21, 25	n/a	1, 5, 7, 10, 11	4, 14	n/a
Bank 23	n/a	2, 3, 8, 9, 16, 18, 20, 21, 25	n/a	1, 5, 7, 10, 11, 22	4, 14	n/a
Bank 24	n/a	2, 3, 8, 9, 16, 18, 20, 21, 25	n/a	1, 5, 7, 10, 11, 22	4, 14	n/a
Bank 25	n/a	2, 3, 8, 9, 16, 18, 20, 21	n/a	1, 5, 7, 10, 11, 22	4, 14	n/a

occassionally 4 or 14 also defaulted in this round. The third round, defaults due to credit loss are 4 and 14, with bank 17 only defaulted once, triggered by initial default of bank 4.

5. After examination (Table 3 on page 13), we found the relative exposure of Bank 9, 12, 14, 18, 20 and 21, $RE_i^1 \preceq 1$, which means their total Tier 1 capital is just enough to cover its total interbank exposure. At the same time, their sizes are small ($size_i \preceq 1\%$ of the total banking sector assets). In addition, bank 22 shares similar characteristics, with $RE_{22}^1 = 2.87$ and $size_i \preceq 1\%$. These all make the above mentioned nodes vulnerable in the network. Hence, the micro and macro analysis conclude the same group of vulnerable nodes in this banking network.

Figure 6: Asset Destroyed% by Direct Counter Party Exposure (Credit Shock). Due to the high capital level of the institutes within the network, defaults caused by credit risk is not high, only less than 5% assets are destroyed due to credit risk.

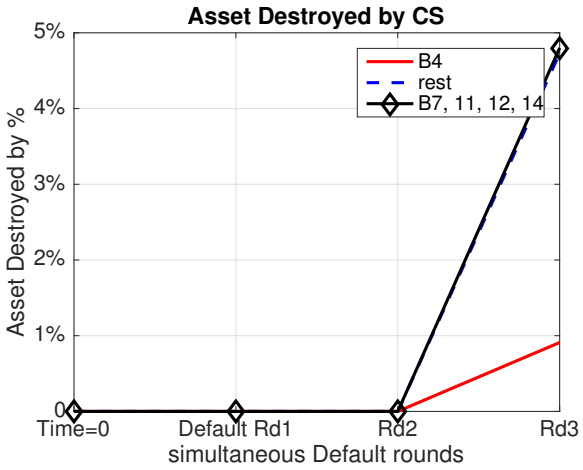

5 Conclusions

Leveraging on the availability of disaggregated interbank exposure data in an advanced emerging market economy, we have used two complementary approaches for analyzing systemic risk in the banking sector. The first approach, the *model-free* approach, examines the topological properties of the network by examining interbank connectivity and exposure using network theory, which does not rely on granular balance sheet information or the funding cost structure faced by the banks. There exist two tails in the connectivity and exposure distribution, which indicates two groups of banks within the network: the well connected money centre banks, and the distant peripheral banks. By the non-targeted, homogeneous capital ratio currently pledged by Basel Committee and implemented by Central banks, banks in our network are solvent and well capitalized. However, using *relative exposure*, a measure developed by Cont et al (2012) [20] to target exposure concentrated banks (SIFIs), a few banks are identified as vulnerable nodes in the network. Also, weighted centrality measure shows the important debtors and creditors in the network.

While the topological analysis is useful for identifying core and peripheral banks, and qualitative measures such as relative exposure and network centrality, systemic risk assessment also requires quantifying the risk. This was accomplished by the *model-based* approach, employing a balance-sheet network framework, to define a specific default mechanism. In this emerging economy, counter-party credit risk, or the *primary effect*, in the interbank market is relatively small, and the default of a single bank does not lead to successive defaults. However, counter-party credit risk is just one of many risk factors driving systemic risk. Results indicate that *secondary effects* such as fire-sale losses, fair value market losses, funding losses and liquidity shortages could lead to a widespread failures in the banking network, which induce further defaults by the domino effect. The default mechanism links liquidity risk and solvency risk by specifying explicitly funding costs and access to funding to banks solvency.

The two complementary approaches single out the same group of SIFIs in the banking network. This finding suggests that a network topology approach could be used when granular public information on balance sheet,

Figure 7: Asset Destroyed% by Funding (Liquidity) Shock. DB-Domestic Banks, FB - Foreign Bank Branches

(a) DB1

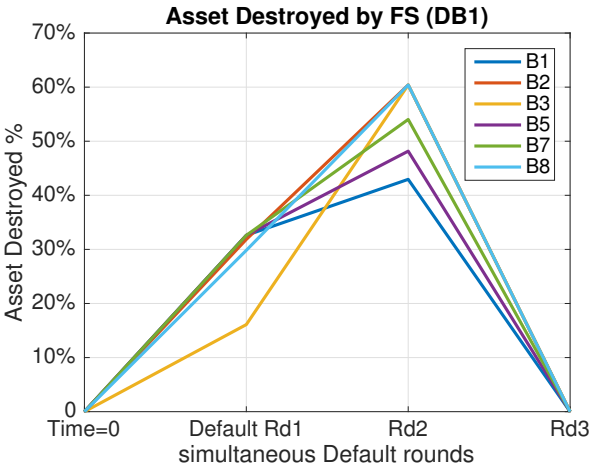

(b) DB2

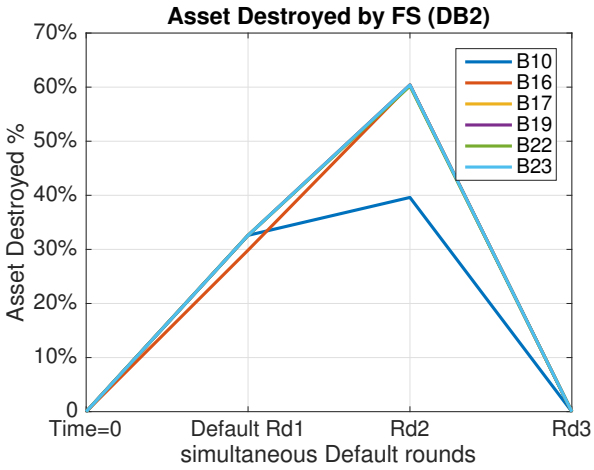

(c) FB1

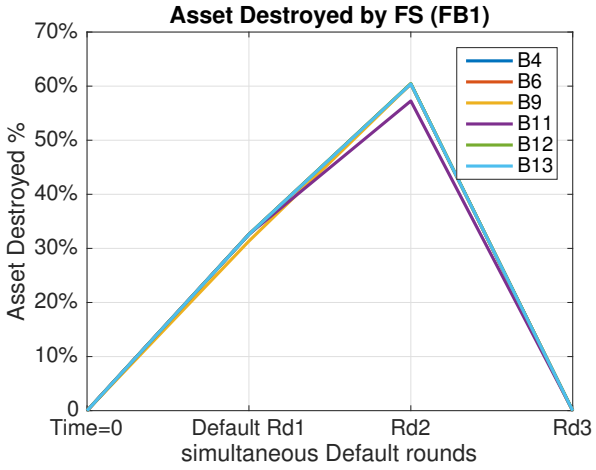

(d) FB2

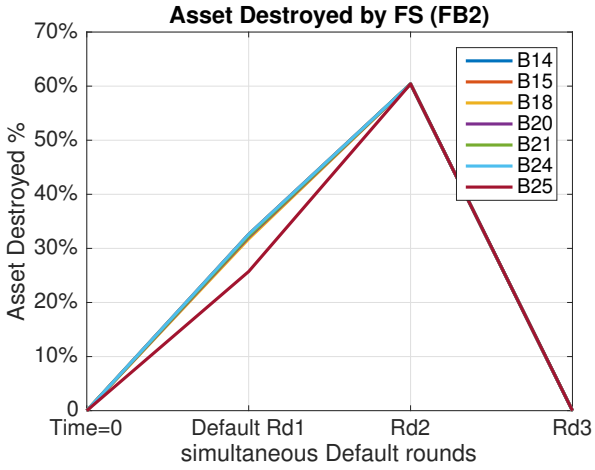

Figure 8: Comprehensive Default Simulation Illustration (CS + FS)

(a) DB1

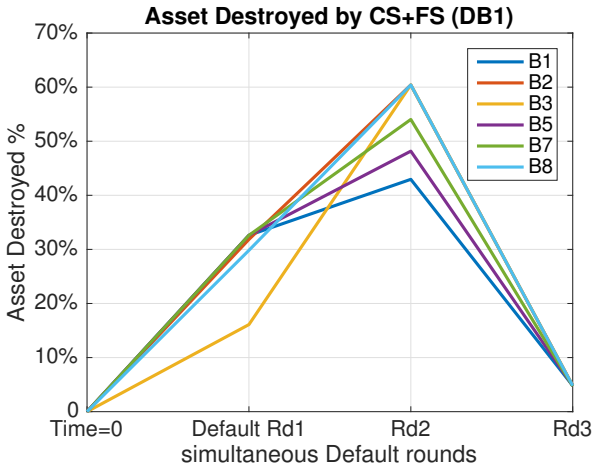

(b) DB2

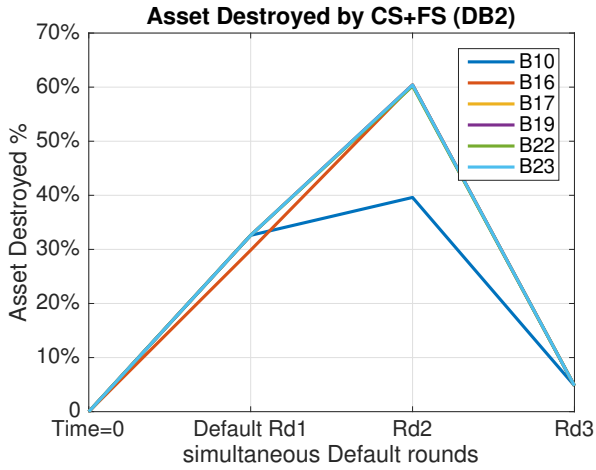

(c) FB1

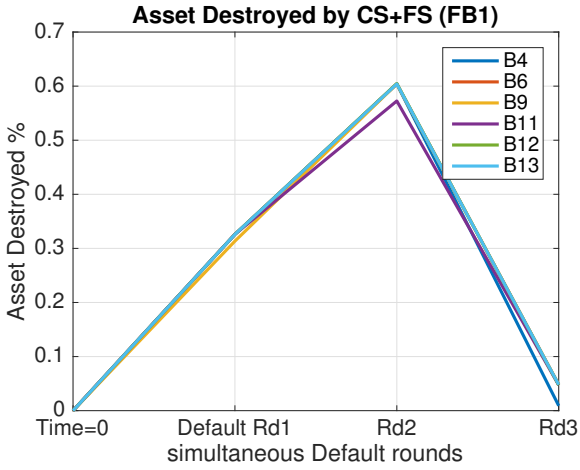

(d) FB2

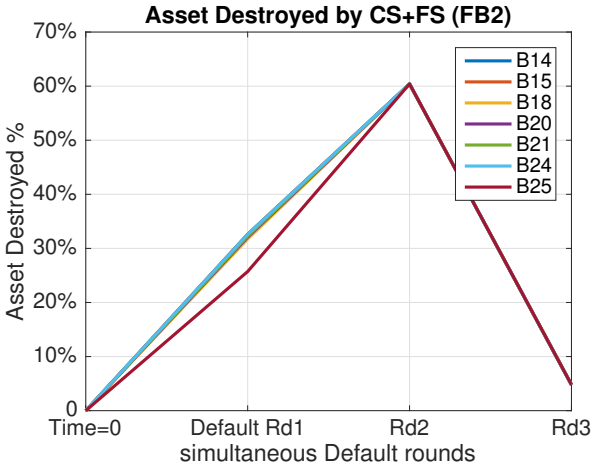

securities prices, and credit ratings is missing. In the case that this information is available, the balance-sheet network approach and default simulations could provide complementary insights on systemic risk. Finally, the analysis highlights the importance of heterogeneous interconnectedness in the banking system as a driver of systemic risk, supporting policy efforts towards incorporating the interconnectedness dimension in the regulatory framework.

6 Appendix I Figures and Tables

Table 9: Shortest path length of the banking network, end-September 2010. The number in cell (i, j) in the table refers to the shortest path length between bank i and bank j. If it is ∞, it means bank i has no access to bank j.

	B1	B2	B3	B4	B5	B6	B7	B8	B9	B10	B11	B12	B13	B14	B15	B16	B17	B18	B19	B20	B21	B22	B23	B24	B25
B1	0	1	1	1	1	1	1	1	1	1	1	1	1	1	1	1	1	1	1	1	1	1	2	∞	1
B2	1	0	1	1	1	2	1	1	1	1	1	1	1	2	2	1	1	1	2	2	1	1	1	∞	1
B3	1	1	0	1	1	1	1	1	1	1	1	1	1	1	1	1	1	1	1	1	1	1	1	∞	1
B4	1	1	1	0	1	1	1	1	1	1	1	1	1	2	2	1	1	1	2	1	2	1	1	∞	1
B5	1	1	1	1	0	2	1	1	1	1	1	1	2	1	1	1	1	1	1	1	1	1	2	∞	1
B6	2	2	1	2	2	0	2	2	2	2	1	2	1	1	2	2	2	2	2	2	2	1	2	∞	2
B7	1	1	1	1	1	2	0	1	1	1	1	1	2	1	2	1	1	1	2	2	1	1	2	∞	1
B8	1	1	1	1	1	2	1	0	1	1	1	1	1	1	1	1	1	1	2	2	1	1	1	∞	1
B9	1	1	1	1	1	2	1	1	0	1	1	1	2	1	1	1	1	1	2	1	2	1	2	∞	1
B10	1	1	1	1	1	1	1	1	1	0	1	1	2	2	1	1	1	1	2	1	2	1	1	∞	1
B11	1	1	1	1	1	1	1	1	1	1	0	1	2	2	1	1	2	1	2	2	2	1	2	∞	1
B12	1	1	1	1	1	2	1	1	1	1	1	0	2	2	1	1	1	1	2	2	2	1	2	∞	1
B13	2	2	1	2	1	2	2	2	2	2	2	2	0	2	2	2	2	2	2	2	2	2	2	∞	2
B14	2	2	1	2	2	2	2	2	2	2	2	2	2	0	1	1	2	2	2	2	2	2	2	∞	2
B15	1	2	1	2	1	2	2	1	1	1	1	1	2	1	0	1	1	1	2	2	2	2	2	∞	1
B16	1	1	1	1	1	2	1	1	1	1	1	1	2	1	2	0	1	1	2	2	1	1	2	∞	1
B17	1	1	1	1	1	2	1	2	2	1	2	2	2	2	2	1	0	1	1	2	1	2	1	∞	1
B18	1	1	1	1	1	2	1	1	1	1	1	1	2	2	1	1	1	0	2	1	1	1	2	∞	1
B19	1	1	2	2	2	2	1	2	2	1	2	2	2	2	2	1	1	2	0	2	2	1	1	∞	1
B20	1	2	1	1	1	2	1	2	1	1	1	2	2	2	2	2	2	2	2	0	2	2	2	∞	2
B21	1	1	1	2	1	2	1	2	2	1	2	2	2	2	2	1	1	2	2	2	0	1	2	∞	1
B22	1	1	1	2	1	2	1	1	1	1	1	1	2	2	2	1	1	1	2	2	1	0	1	∞	1
B23	1	1	1	1	1	1	1	1	1	1	1	1	1	1	1	1	1	1	1	1	1	1	0	∞	1
B24	∞	∞	∞	∞	∞	∞	∞	∞	∞	∞	∞	∞	∞	∞	∞	∞	∞	∞	∞	∞	∞	∞	∞	0	∞
B25	1	1	1	1	1	2	1	1	1	1	1	1	2	2	1	1	1	1	2	1	1	1	2	∞	0

7 Appendix II Statistical Methodology

7.1 Normal Laplace distribution and double pareto-lognormal distribution

The *dPlN* distribution has four parameters, which is similar to log-hyperbolic distribution first developed by . The *dPlN* and log-hyperbolic both exhibit power-law behavior in both tails. These two distributions are derived from mixture of lognormal distributions. The difference between the two is that *dPlN* arises from the distribution of a final state of a *Geometric Brownian Motion (GBM)* with a constant killing rate, while the hyperbolic distribution has a more complicated killing rate functions. Consider a *Geometric Brownian Motion (GBM)* defined by *Itô stochastic differential equation (SDE)* as follows:

$$dX = \mu X dt + \sigma X dw \tag{8}$$

It has an initial state $X(0) = X_0$ distributed lognormally, $logX_0 \sim N(\upsilon,\, \sigma^2)$. After T units of time, $X(T)$ will have a lognormal distribution as follows:

$$logX(T) \sim N(\upsilon + (\mu - {\sigma^2}/{2})T,\, \tau^2 + \sigma^2 T) \tag{9}$$

Supposedly at time T, the *GBM* process is observed has an exponentially distributed random variable with density $f_T(t) = \lambda e^{-\lambda t}$, $t > 0$. λ is refereed as the "killed" rate rate, and $k(X) \equiv \lambda$. The distribution of the state $\hat{X}$ at the time of the observation of the "killing", is a mixture of lognormal random variables 7.1with mixing parameter T.

Taking logarithmic of X, $\hat{Y} = log(\hat{X})$ so that $\hat{Y}$ is the state of an ordinary Brownian motion after an exponentially distributed time. Y is the sum of independent variables W and Z. $Z \sim N(\upsilon,\, \tau^2)$; W is a skewed Laplace distribution as described by , with a *pdf* as follows:

$$fw(\omega) = \begin{cases} \frac{\alpha\beta}{\alpha+\beta} e^{\beta\omega},\ for\, \omega \leq 0 \\ \frac{\alpha\beta}{\alpha+\beta} e^{-\alpha\omega},\ for\, \omega \geq 0 \end{cases} \tag{10}$$

where α and β are roots of characteristic function

$$\frac{\sigma^2}{2} z^2 + (\mu - \frac{\sigma^2}{2}) z - \lambda = 0 \tag{11}$$

Hence, the distribution of $\hat{Y}$ is a convolution of Laplace and normal distributions. We introduce the concept of *Mill's ratio* for convenience as follows:

$$R(z) = \frac{\Phi^c(z)}{\phi(z)} \tag{12}$$

where $\Phi^c(z)$ is the complementary cumulative density function of normal distribution, and $\phi(z)$ is the normal pdf. We can then express the density function of $\hat{Y}$ as follows:

$$g(y) = \frac{\alpha\beta}{\alpha+\beta} \phi(\frac{y-\upsilon}{\tau})[R(\alpha\tau - (y-\upsilon)/\tau) + R(\beta\tau + (y-\upsilon)/\tau)] \tag{13}$$

This is a *Normal-Laplace (N-L)* distribution. In other words, $Y \sim NL(\alpha, \beta, \nu, \tau^2)$.

Since a Laplace random variable can be expressed as the difference between two exponentially distributed variates, we can rewrite Y as follows:

$$Y \doteq \nu + \tau Z + {E_1}/{\alpha} - {E_2}/{\beta} \tag{14}$$

where E_1 and E_2 are standard independent exponentiate deviates, and Z is a standard normal deviate, which is independent of E_1 and E_2. One can use this equation to generate pseudo-numbers from N-L distribution.

We then deduce the *pdf* of $\hat{X}$ as follows:

$$f(x) = \frac{1}{x} g(log(x)) \tag{15}$$

That is, in the form of *ccdf* $\phi_c$and *pdf* ϕ of standard normal distribution $N(0,1)$ as follows:

$$f(x) = \frac{\alpha\beta}{\alpha+\beta}[A(\alpha,\upsilon,\tau)x^{-\alpha-1}\Phi(\frac{logx - \upsilon - \alpha\tau^2}{\tau}) + x^{\beta-1}A(-\beta,\upsilon,\tau)\Phi^c(\frac{logx - \upsilon + \beta\tau^2}{\tau})] \tag{16}$$

where

$$A(\theta, \upsilon, \tau) = exp(\theta\upsilon + {}^{\alpha^2\tau^2}/_2) \tag{17}$$

This is a double Pareto lognormal distribution. In other words, $X \sim dPlN(\alpha, \beta, \upsilon, \tau^2)$. From 7.1, we can express X as follows:

$$X \doteq {}^{UV_1}/_{V_2} \tag{18}$$

Where U follows a lognormal distribution that $log(U) \sim N(\upsilon, \tau^2$, and $V_1$and V_2 are Pareto distributed and with a *pdf* as follows:

$$f(\upsilon) = \theta\upsilon^{-\theta-1}, \upsilon > 1 \tag{19}$$

with $\theta = \alpha$ and $\theta = \beta$ for $V_1$and V_2, respectively. We can rewrite the expression for X as

$$X \doteq UQ \tag{20}$$

where $Q = \frac{V_1}{V_2}$, and has *pdf* as follows:

$$f(q) = \begin{cases} \frac{\alpha\beta}{\alpha+\beta} q^{\beta-1} & for\, 0 < q < 1 \\ \frac{\alpha\beta}{\alpha+\beta} q^{-\alpha-1} & for\, q < 1 \end{cases} \tag{21}$$

This is referred to as the *double pareto-lognfrmal (dPlN) distribution.* One can generate pseudo-numbers from dPlN distribution by exponentiating the N-L pseudo-numbers generated using 7.1.

7.2 Properties of N-L distribution

There are two special cases of the N-L distribution:

1. When $\alpha = \infty$. This corresponds to the case of N-L distribution is the difference between the independent normal and exponential components. It exhibits extra normal behavior in the lower tail. It is also referred to as the *right-handed normal-exponential distribution*, and is expressed as $Y \sim NE_r(\beta, \upsilon, \tau^2)$. Its *pdf* is reduced from the original 7.1:

$$g_1(y) = \beta\phi(\frac{y-\upsilon}{\tau})R(\beta\tau + (y-\upsilon)/\tau) \tag{22}$$

2. When $\beta = \infty$. This corresponds to the case of N-L distribution is the sum of the independent normal and exponential components. It exhibits extra normal behavior in the upper tail. It is often referred to as *left-handed normal-exponential distribution*, and is expressed as $Y \sim NE_l(\alpha, \upsilon, \tau^2)$. Its *pdf* is

$$g_2(y) = \alpha\phi(\frac{y-\upsilon}{\tau})R(\alpha\tau + (y-\upsilon)/\tau) \tag{23}$$

The $N - L(\alpha, \beta, , \upsilon, \tau^2)$ distribution can be represented as a mixture of the *right-handed* and *left-handed normal-exponential distributions*, and its pdf can be written as follows:

$$g(y) = \frac{\beta}{\alpha+\beta} g_1(y) + \frac{\beta}{\alpha+\beta} g_2(y) \tag{24}$$

The *cumulative density function (cdf)* of the $N - L(\alpha, \beta, , \upsilon, \tau^2)$ can be expressed as follows:

$$G(y) = \Phi(\frac{y-\upsilon}{\tau}) - \phi(\frac{y-\upsilon}{\tau})\frac{\beta R(\alpha\tau - (y-\upsilon)/\tau) + \alpha R(\beta\tau + (y-\upsilon)/\tau)}{\alpha+\beta} \tag{25}$$

The *moment generating function (mgf)* of the $N - L(\alpha, \beta, , \upsilon, \tau^2)$ is the product of the *mgf* normal and exponential components, and can be expressed as follows:

$$M_Y(s) = \frac{\alpha\beta\, exp(\upsilon s + {}^{\tau^2 s^2}/_2)}{(\alpha - s)(\beta + s)} \tag{26}$$

7.3 The properties of dPlN distribution

Corresponding to the two cases (right-handed and left-handed) of the *N-L distribution* described as above, we deduce the

right-handed and *left-handed dPlN distribution pdf* as follows:

1. When $\alpha = \infty$. This limiting *single Pareto-lognormal* distribution only exhibits heavy tail behavior in the lower tail.

$$f_1(x) = \beta x^{\beta-1} A(\beta, \upsilon, \tau)\Phi(\frac{log\, x - \upsilon + \beta\tau^2}{\tau}) \tag{27}$$

2. When $\beta = \infty$. This limiting *single Pareto-lognormal* distribution only exhibits heavy tail behavior in the upper tail.

$$f_2(x) = \alpha x^{-\alpha-1} A(\alpha, \upsilon, \tau)\Phi(\frac{log\, x - \upsilon - \alpha\tau^2}{\tau}) \tag{28}$$

where $A(\theta, \upsilon, \tau) = exp(\theta\upsilon + {}^{\alpha^2\tau^2}/_2)$ as in the case of *N-L* distribution.

3. The *dPlN* distribution *pdf* can be represented as a mixture of *right-handed* and *left-handed* pareto-lognfrmal distributions:

$$f(x) = \frac{\beta}{\alpha+\beta} f_1(x) + \frac{\alpha}{\alpha+\beta} f_2(x) \tag{29}$$

The cdf of the dPlN distributions can be written as $F(x) = G(exp(x))$, where G is equal to 25, or it can be expanded in the forms of ϕ and Φ^c as follows:

$$F(x) = \Phi(\frac{logx - \upsilon}{\tau}) - \frac{1}{\alpha+\beta}[\beta x^{-\alpha} A(\alpha, \upsilon, \tau)\Phi(\frac{logx - \upsilon - \alpha\tau^2}{\tau}) + \alpha x^{\beta} A(-\beta, \upsilon, \tau)\Phi^c(\frac{logx - \upsilon - \beta\tau^2}{\tau})] \tag{30}$$

The $dPlN(\alpha, \beta, \upsilon, \tau^2)$ exhibits heavy tail behavior at both tails in the sense that

$$f(x) \sim k_1 x^{-\alpha-1} (x \to \infty) \tag{31}$$

and

$$f(x) \sim k_2 x^{\beta-1} (x \to 0) \tag{32}$$

where

$$k_1 = \alpha A(\alpha, \upsilon, \tau) \tag{33}$$

and

$$k_2 = \alpha A(\beta, \upsilon, \tau) \tag{34}$$

The maximum likelihood function of *dPlN* and the *N-L* distributions are the same, in the sense that if the dataset $(x_1, x_2, x_{3,\dots} x_n)$ is assumed to follow a *dPlN*, then its logarithmic form $(y_1, y_2, , \dots, y_n)$ is assumed to follow a *N-L* distribution. The log likelihood function is as follows:

$$l(\alpha, \beta, \tau) = nlog\alpha + nlog\beta - nlog(\alpha+\beta) + \sum_{i=1}^{n} log[R(\alpha\tau - \frac{y_i - \bar{y} + {}^1/_\alpha + {}^1/_\beta}{\tau}) + R(\beta\tau + \frac{y_i - \bar{y} + {}^1/_\alpha + {}^1/_\beta}{\tau})] \tag{35}$$

and υ can be solved analytically as $\hat{\upsilon} = \bar{y} - {}^1/_\alpha + {}^1/_\beta$.

References

[1] Acharya, V., Pedersen, L., Philippon, T., and Richardson, M. (2010). Measuring systemic risk. Working paper.

[2] Allen, F., and Gale, D. (2000). "Financial contagion." *Journal of Political Economy* 108, no. 1: 1-33.

[3] Anderson, T. W., Darling, D. A. (1952). "Asymptotic theory of certain "goodness-of-fit" criteria based on stochastic processes". *Annals of Mathematical Statistics* 23: 193–212. doi:10.1214/aoms/1177729437

[4] Armantier, Olivier and Adam Copeland (2012).*Federal Reserve Bank of New York Staff Reports*, no. 575, October.

[5] Arnold, B. C., 1983, *Pareto Distributions* (International Cooperative Publishing House, Fairland, Maryland).

[6] Barabasi A-L., Albert R. (1999). “Emergence of Scaling in Random Networks”. *Science* Vol 286.

[7] Basel Committee on Banking Supervision (2013). *Global Systemically Important Banks: Updated Assessment Methodology and the Higher Loss Absorbency Requirement.*

[8] Billio, M., M. Getmansky, A. W. Lo, and L. Pelizzon (2010). "Econometric measures of systemic risk in the finance and insurance sectors." *NBER Working Paper* 16223.

[9] Bank for International Settlements (BIS) (1994). *64th Annual Report*. Basel, Switzerland: BIS.

[10] Bisias, Dimitrios, Mark Flood, Andrew W. Lo, and Stavros Valavanis (2012). "A Survey of Systemic Risk Analytics." *Office of Financial Research Working Paper*.

[11] Board of Governors of the Federal Reserve System. 2001. *Policy Statement on Payments System Risk, Docket* No. R-1107, 1–13. Washington, D.C., May 30.

[12] Boss, M., Elsinger, H., Lehar, A., and Summer, M. (2004). *The network topology of the interbank marke*t. *Quantitative finance*, 4: 677-684.

[13] Brunnermeier, Markus K., Charles Goodhart, Andrew Crockett, Avinash Persaud, and Hyun Song Shin, 2009a, The Fundamental Principles of Financial Regulation. *Geneva Report on the World Economy*.

[14] Brunnermeier, Markus.K., and Lasse.H. Pedersen (2009b). Market liquidity and funding liquidity. *Review of Financial Studies*, Vol. 22, No. 6, pp. 2201-2238.

[15] Chan-Lau, Jorge A. (2010). "Balance Sheet Network Analysis of Too-Connected-to-Fail Risk in Global and Domestic Banking Systems." *IMF Working Paper*.

[16] Chan-Lau, Jorge A., Chienmin Chuang, Jin-Chuan Duan, and Wei Sun, 2016, “Banking Network and Systemic Risk via Forward-Looking Partial Default Correlations,” working paper, International Monetary Fund and National University of Singapore.

[17] Chan-Lau, Jorge A., and Amadou N.R. Sy (2007). Distance to Default in Banking: A Bridge Too Far? *Journal of Banking Regulation*, Vol. 9, No. 1 pp. 14 - 24.

[18] Choromański, K.; Matuszak, M.; MięKisz, J. (2013). "Scale-Free Graph with Preferential Attachment and Evolving Internal Vertex Structure". *Journal of Statistical Physics* 151 (6): 1175. doi:10.1007/s10955-013-0749-1.

[19] Clauset, Aaron, Shalizi, Rohilla, Cosma, Newman, M.E.J. (2009). Power-law distributions in empirical data *SIAM Review*, Vol.51, No.4, pp.661-701

[20] Cont, Rama, A. Moussa, Santo, E. B. (2012). Network structure and systemic risk in banking systems.

[21] Degrysea, Hans, and Gregory Nguyen (2007). "Interbank Exposures: An Empirical Examination of Contagion Risk in the Belgian Banking System." *International Journal of Central Banking* 2007: 123-171.

[22] ECB (2010). "Financial networks and financial stability." *Financial Stability Review*, 2010: 155-160.

[23] Edwards Franklin, and Frederic S. Mishkin (1995). "The Decline of Traditional Banking: Implications for Financial Stability and Regulatory Policy." *Federal Reserve Bank of New York, Economic Policy Review* 1, no. 2, pp. 27-45.

[24] Eisenberg, L., and T. Noe (2001). "Systemic Risk in Financial Systems." *Management Science* 47, pp. 236-249.

[25] Elsinger, Helmut, Alfred Lehar, and Martin Summer (2006a). "Risk Assessment for Banking Systems." *Management Science* 52, no. 9, pp. 1301-1314.

[26] Elsinger, Helmut, Alfred Lehar, and Martin Summer (2006b). "Using market information for banking for systemic risk assessment." *International Journal of Central Banking* 2, no. 1, pp. 137-165.

[27] Erdős, P. Rényi, A (1959) "On Random Graphs I" in Publ. Math. Debrecen 6, p. 290–297.

[28] Merill, C., T. Nadauld, R. Stulz, and S. Sherlund, 2013, "Why were there fir sales of mortgage-backed securities by financial institutions during the financial crisis," working paper, Brigham Young University, Ohio State University, and the Board of Governors of the Federal Reserve.

[29] Friedman Milton, and Anna Jacobson Schwartz (1963). A Monetary History of the United States, 1867-1960. *Princeton University Press*.

[30] Furfine, C.H. (2003) "Interbank exposure: quantifying the risk of contagion." *Journal of Money, Credit and Banking* 35 , no. 1: 111-128.

[31] Gorton, Gary (2010). *Slapped by the Invisible Hand: the Panic of 2007*. Oxford University Press.

[32] Group of Ten (2001). "Report on Consolidation in the Financial Sector: Chapter III. Effects of consolidation on financial risk." *International Monetary Fund Working Paper*.

[33] Haldane, Andrew G (2009). "Rethinking the financial network." *Amsterdam: Financial Student Association*, 2009.

[34] Hill, B. M. (1975). *Annals of Statistics* vol 3, 1163.

[35] Jo, Jae Hyun (2012). "Managing systemic risk from the perspective of the financial network under macroeconomic distress." *Financial Stability Institute*.

[36] Kaufman, George G. (1995). Comments on Systemic Risk, *Research in financial services*, *banking, financial markets and systemic risks.* vol 7. edited by George G. Kaufman, 47–52. Greenwich, Conn.: JAI.

[37] Kirilenko, Andrei, Albert S. Kyle, Mehrdad Samadi, and Tugkan Tuzun, 2014, "The Flash Crash: the Impact of High Frequency Trading on an Electronic Market," working paper, CFTC.

[38] Institutions. Congressional Research Service, 2015

[39] Luce, R. Duncan; Perry, Albert D. (1949), "A method of matrix analysis of group structure", *Psychometrika* 14 (2): 95–116, doi:10.1007/BF02289146.

[40] Mishkin, Frederic S. (1994) "Preventing financial crisis: An international perspective." *National Bureau of Economic Research*.

[41] Mitchell, M., and T. Pulvino (2010), "Arbitrage crashes and the speed of capital," working paper.

[42] Mitzenmacher, M. Dynamic models for file sizes and double Pareto distributions. 2001, Draft manuscript avilable at http://www.eecs.harvard.edu/ michaelm/NEWWORK/papers/.

[43] Newman, M. E. J. (2003) "The structure and function of complex networks".

[44] Onnela, J. P, Saramaki, J., Hyvonen, J., Szabo, G., Lazer, D., Kaski, K., Kertesz, J. and Barabasi, A. -L. (2007). Structure and tie strengths in mobile communication networks. *Proceedings of the National Academy of Sciences* 104 (18): 7332–7336. doi:10.1073/pnas.0610245104.

[45] William J. Reed, Murray Jorgensen (2004). The double Pareto lognormal distribution - a new parametric model for size distributions, *Communications in Statistics Theory and Methods*, Vol. 33, No. 8, pp. 1733-1753.

[46] Roukny, T., Georg, C. and Battiston, S (2014). A network analysis of the evolution of the German interbank market, *Deutsche Bundesbank discussion paper* No 22/2014.

[47] Sheldon, G. and Maurer, M. (1998). Interbank lending and systemic risk: An empirical analysis for switzerland. *Swiss Journal of Economics and Statistics*, 134(IV):685-704.

[48] Upper, Christian (2011). "Simulation methods to assess the danger of contagion in interbank markets." *Journal of Financial Stability* (Elsevier): 15-30.

[49] Upper and Worm (2004) Upper, Christian & Worms, Andreas, 2004. "Estimating bilateral exposures in the German interbank market: Is there a danger of contagion?," *European Economic Review*, Elsevier, vol. 48(4), pages 827-849, August.

[50] Wasserman, S., and Faust, K. (1994). *Social Network Analysis: Methods and. Applications*. Cambridge, ENG and New York: Cambridge University Press.

[51] Watts D. J., Strogatz S. (June 1998). "Collective dynamics of 'small-world' networks". Nature 393 (6684): 440–442. Bibcode:1998Natur.393..440W. doi:10.1038/30918. PMID 9623998.

[52] Wells, Simon (2004). "Financial interlinkages in the United Kingdom's interbank market and the risk of contagion." Bank of England Working Paper 230 (2004).

[53] Zipf GK (1949). Human Behavior and the Principle of Least Effort. Cambridge, Massachusetts: Addison-Wesley. p. 1.

[54] Zhou, H., Huang, X., and Zhu, H. (2009). A framework for assessing the systemic risk of major financial institutions. *Journal of Banking and Finance*, 2036-2049:2036{2049.